Marine Pollution Bulletin 172 (2021) 112717

Contents lists available at ScienceDirect

Marine Pollution Bulletin

journal homepage: www.elsevier.com/locate/marpolbul

Drill cuttings and drilling fluids (muds) transport, fate and effects near a coral reef mesophotic zone

Ross Jones *, Mary Wakeford, Leanne Currey-Randall, Karen Miller, Hemerson Tonin

Australian Institute of Marine Science Perth (Western Australia), Townsville, Queensland, Australia

ARTICLE INFO

Keywords:
Mesophotic reef
Water based drilling fluid
Drilling mud
Cuttings
Near field model
Hindcast modelling

ABSTRACT

The study was conducted to improve knowledge and provide guidance on reducing uncertainty with impact predictions when drilling near sensitive environments. Near/Far-field hindcast modelling of cuttings/drilling fluid (mud) discharges from a floating platform was conducted, based on measured discharge amounts and durations and validated by ROV-based plume and seabed sampling. The high volume, concentration, and discharge rate water-based drilling mud discharges (mud pit dumps) were identified as the most significant dispersal risk, but longer-range movement was limited by the generation of jet-like plumes on release, which rapidly delivered muds to the seabed (80 m). Effects to the sparse benthic filter feeder communities close to the wells were observed, but no effects were seen on the epibenthic or demersal fish assemblages across the nearby mesophotic reef. For future drilling near sensitive environments, the study emphasized the need to better characterise drilling fluid discharges (volumes/discharge rates) to reduce uncertainty in modelling outputs.

1. Introduction

Australia's North West Shelf marine region is a significant hydrocarbon province accounting for 90% of current Australian offshore oil and gas production (Commonwealth of Australia, 2010). The region also contains unique environmental assets including open water emergent coral reefs and many submerged banks and shoals (Commonwealth of Australia, 2012; Wilson et al., 2019). There are many examples of a close association between hydrocarbon deposits and these genetically-rich communities, presenting a unique and well recognized conservation challenge for successful exploration and extraction (International Risk Consultants, 2007; May, 1992; O'Brien et al., 2002; Richert et al., 2015; Vince et al., 2015).

The Greater Western Flank Phase 2 development of Woodside Energy Limited exemplifies this challenge. Located 150 km off the Australian west coast, one of the hydrocarbon fields, the Lady Nora and Pemberton lies very close to Rankin Bank, a submerged reef with a deeper surrounding mesophotic coral ecosystem. Drilling generates waste in the form of drill cuttings and drilling fluids (muds) (Bakke et al., 2013; Cordes et al., 2016; Ellis et al., 2012; Holdway, 2002; IOGP, 2003, 2016, 2021). These are effectively seawater slurries of solid particles (crushed sedimentary rock) of various sizes and densities. Drilling fluids also contain numerous solid and liquid additives including lubricants, detergents, emulsifiers, defoamers, foaming agents, bactericides and corrosion inhibitors (Hinwood et al., 1994; Khondaker, 2000; Melton et al., 2000). However, the bulk of the additives include pre-hydrated bentonite (a viscosifier), barite (the mineralogical name for $BaSO_4$ used as a weighting agent), and potassium chloride (to inhibit clay hydration). In Australia, cuttings and some types of drilling fluids (water-based drilling fluids) are routinely discharged below the sea surface (IOGP, 2016, 2021; Neff, 2010), and their ultimate fate is the seabed (Durgut et al., 2015; Melton et al., 2000).

An important consideration for all discharges from oil and gas exploration and production activities is ecological impact (Cordes et al., 2016) and a basic task in all environmental impact assessments and a fundamental precept in management policies for marine discharges is defining the size of the area at risk (EPA, 2011; IOGP, 2016, 2021; NOPSEMA, 2018). The prediction and associated environmental management programs form the basis for a judgement by the regulator about environmental acceptability. When predicting the transport and fate of drilling discharges at the impact assessment stage there are usually many unknowns, from fundamental information such as the timing of the proposed drilling and even the nature of the drilling platform, to more exact information such as the drill bit diameters and interval lengths and the mud systems to be used. Generalizations or approximations of what is expected to occur are used; however, as noted by Rye

* Corresponding author.
E-mail address: r.jones@aims.gov.au (R. Jones).

https://doi.org/10.1016/j.marpolbul.2021.112717
Received 11 March 2021; Received in revised form 6 July 2021; Accepted 8 July 2021
Available online 9 August 2021

and Furuholt (2010), the predictive ability of models is very much related to the input data. Any divergence will result in uncertainty of model outputs and assumed amounts of discharges often differ from actual discharges (Pivel et al., 2009).

The objective of this study was to increase confidence in outputs of plume dispersion modelling identifying where, if possible, improvements could be made for environmental management of future drilling campaigns around sensitive environments. The study involved hindcast modelling of the Lady Nora and Pemberton drilling campaign where three wells were drilled in close proximity using an anchored, semi-submersible mobile offshore drilling rig and with all cuttings and drilling fluid (mud) discharges through a submarine outfall.

Information on the discharge volumes and chronology of discharges were closely scrutinised with particular attention to high volume, high emission rate (sensu Ayers et al., 1982) drilling fluid discharges (mud pits dumps, see below) as they have a greater potential for longer-range transport. Drilling mud and cuttings samples were collected and characterised, and the information used together with in situ oceanographic data as input parameters for a coupled near and far field model plume dispersion model. Fieldwork during the drilling program involved measuring and profiling suspended solids (TSS) concentrations in discharges under the drilling rig by a remotely operated vehicle (ROV),

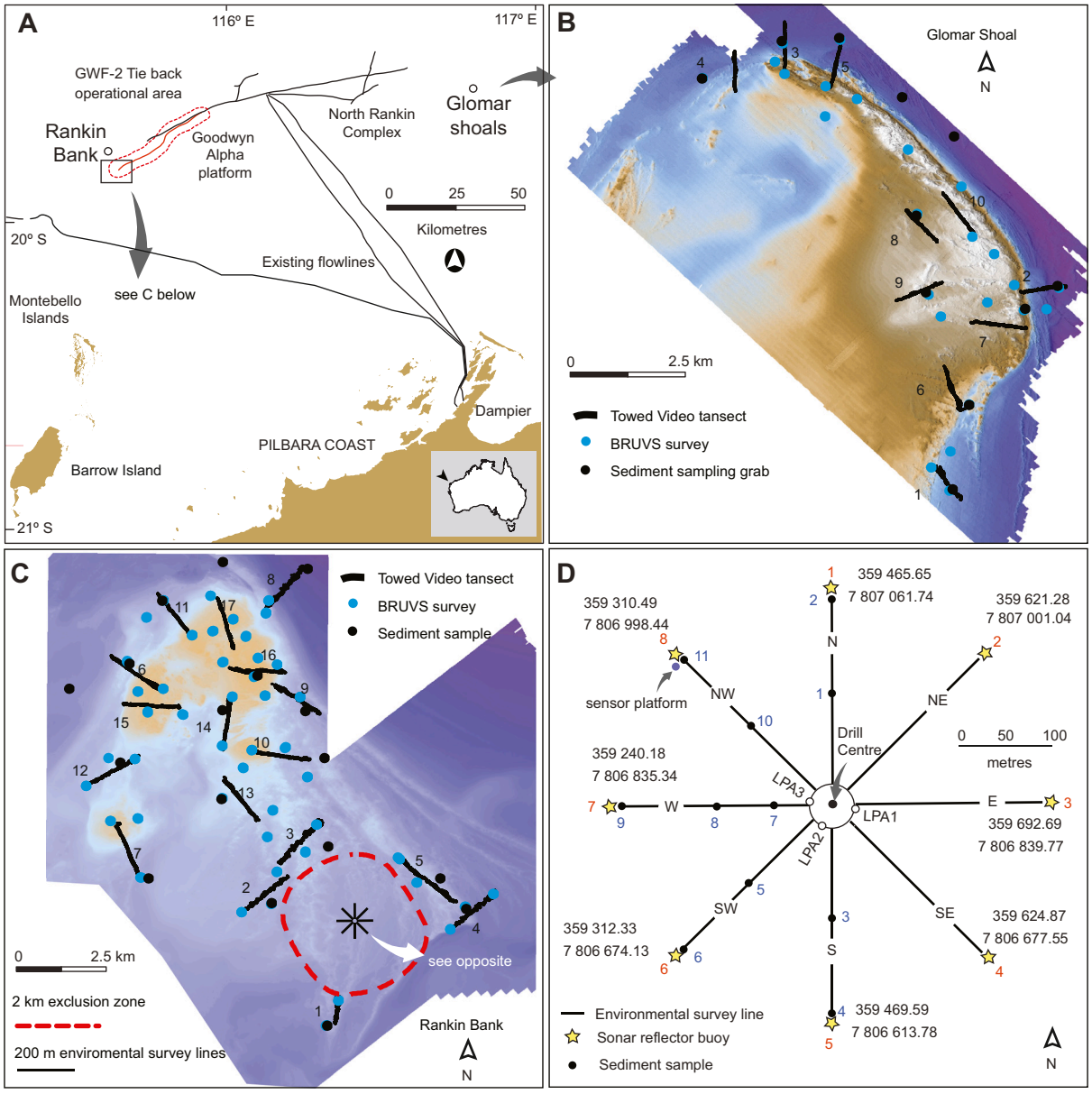

Fig. 1. Location maps showing (A) the Greater Western Flank (GWF-2) development off the Pilbara coast of Western Australia on the SE flank of Rankin Bank (−19.777708°, 115.620706°), and the location of Glomar Shoal (−19.560611°, 116.795172°) 125 km ENE of Rankin Bank which was used as a reference site, (B and C) location of the ship-based towed video, baited remote underwater video stations (BRUVS) surveys and sediment sampling sites on Rankin Bank and Glomar Shoal, (D) location of the Lady Nora Pemberton (LPA) LPA1, LPA2 and LPA3 wells, the centre point of which (−19.829416°, 115.658084°) was referred to as the 'drill centre' and used for all distance calculations. A total of 8 sonar contact buoys were temporarily installed at cardinal and intercardinal points 200 m away from the drill centre and were used for ROV-based seabed surveys and sediment sampling. A seabed mounted sensor platform was also located at the end of transect line 8. After the installation of the buoys at the desired location, a number of ultra-short baseline fixes were taken of the ROV, with the centre of the ROV's bumper as close as possible to the sonar buoy weight. For all spatial analysis Transverse Mercator UTM Zone 50 WGS84 was used. ArcGIS datum transformations were applied to all data sets not on WGS84 to align with existing WGS84 surveys. (For interpretation of the figure legend, the reader is referred to the web version of this Figure which is in color).

characterising seabed samples for sediment particle size distributions and chemical content using barium as a tracer of discharges. Pre- and post-drilling surveys of epibenthic communities were conducted close to the wells using high definition cameras mounted to the ROV. Ship-based towed video surveys and surveys of demersal fish communities were also conducted before and after drilling across Rankin Bank. The model predictions were then compared to empirical measurements — which corresponds to hindcast modelling of the drilling campaign (Nedwed et al., 2006; Pivel et al., 2009; Rye et al., 2006; Zhao et al., 2011). Collectively, the analyses provided a clear, coherent story of the effects of the discharges on the surrounding environment, the size and scale of the area influenced, and how to increase surety in predictions when modelling the movement of drilling fluid discharges.

1.1. Rankin Bank and Glomar Shoal

The Lady Nora and Pemberton hydrocarbon field is located on the SE flank of Rankin Bank (Fig. 1C) approximately 150 km north-west of the town of Dampier on the Pilbara coast of north-west Western Australia (Fig. 1A). Rankin Bank and Glomar Shoal (hereafter 'Rankin' and 'Glomar') are the only large, complex, bathymetrical features on the outer western shelf of the West Pilbara (Wilson, 2013). Rankin rises up from a 80–120 m deep relatively homogenous sedimentary continental shelf environment to a series of rugose peaks and plateaus 20–40 m from the surface (Abdul Wahab et al. (2018)). The shallower (<40 m) areas support a diverse coral reef ecosystem with hard coral cover of 20–25%. The deeper surrounding area supports a mesophotic coral ecosystem characterised by a gradient of declining light availability and a gradual community transition from phototrophic to mixotrophic and heterotrophic communities (Abdul Wahab et al., 2018; Lesser et al., 2009; Loya et al., 2016). A photomosaic of Rankin habitats showing the position of the drilling activities and representative images of the epibenthos at different depths is available in the supplementary material (S1). Rankin is much shallower than Glomar which plateaus at ~40 m and on account of the different bathymetry and substrate type has 10× more coral cover 30× more cover of benthic taxa in general, 2× the abundance of fish and 1.5× the fish diversity than Glomar (Abdul Wahab et al., 2018).

Both Rankin and Glomar share a number of similarities to other shoals on the North West Shelf (Heyward et al., 2012; Moore et al., 2017) but are highly isolated, and located ~1000 km from the nearest similar feature (Echuca Shoal, Abdul Wahab et al. (2018)). They represent 'islands' of solid reef structure in an otherwise relatively homogenous environment and are biodiversity hotspots and because of local enhanced productivity support significant numbers of fish including commercially and recreationally important species (DEWHA, 2008). By sharing species with emergent reef ecosystems in the region, they could act as refuges, buffering disturbances to shallow-water environments. Rankin and Glomar have both have been recognized as very important features for the region's biodiversity and ecosystem function and integrity (Abdul Wahab et al., 2018; Falkner et al., 2009; Hayes et al., 2015).

1.2. Greater Western Flank-2 (GWF-2) Lady Nora Pemberton (LPA) drilling campaign

Three wells were considered optimal for maximising gas recovery from the fields and were batch drilled in multiple segments including 42″, 26″, 17.5″, 12.25″ and 8.5″ hole diameter sections using a moored, semi-submersible mobile offshore drilling unit (hereafter MODU). The wells were ultimately tied back via subsea flowlines to the Goodwyn Alpha platform/facility (Fig. 1A). Batch drilling involves completing the same section of each of the 3 wells before drilling the next deeper sections. This necessitated repeated moving (kedging) of the MODU between wells using the anchoring system, and continual repositioning of the blow out preventer (BOP) (see Fig. 2A). The anchoring points were up to 2 km away from the MODU and a vessel exclusion zone was

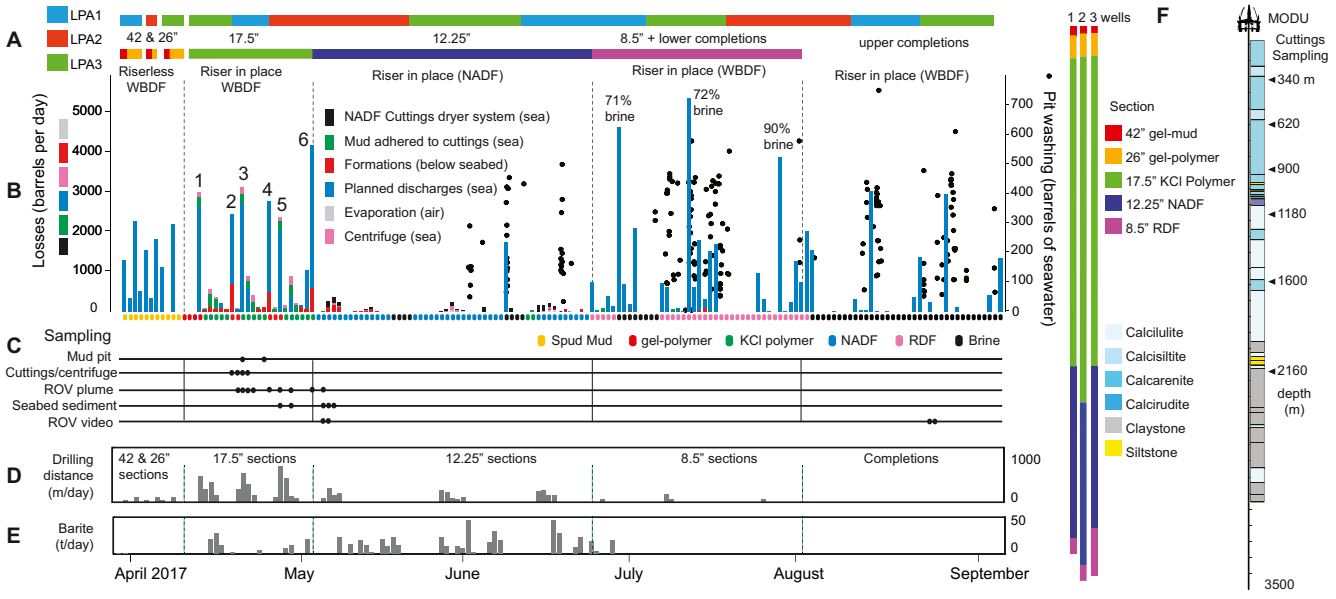

Fig. 2. Schematic representation of the drilling program showing: (A) movement (kedging, indicated by arrows) of the MODU between the 3 LPA wells during the batch drilling process, (B) daily fluid discharges (US barrels, vertical bars) and pit cleaning discharges (US Barrels, white circles) and main mud type used, (C) timing of the various sampling activities, (D) distance (m) drilled each day, (E) Barite (t) used each day (F) vertical representation of the drilling campaign showing predicted lithology and average depths of the sections and drilling fluid used and depth of the cuttings samples collected from the shale shakers at 340 to 2317 m during the drilling of the 17.5″ section of LPA1. The numbers 1–6 above the discharges in the 17.5″ sections refer to loss of discrete high volume, high rate, mud pit discharge events of WBDFs. Note that 'NADF cutting dryer system losses' refers to NADF discharge as mud still adhered to cuttings, but cuttings discharge was only permitted if the average oil content was <10% wt/wt (on dry cuttings) after passing the wet NADF cuttings through the cuttings dryer system. NADF may also enter the marine environment after washing mud pits which have previously contained NADF, although discharge was only allowed if with the oil by volume content of the washings was <1%. An additional loss of drillings muds was by deck washing but all desk washing was collected in tanks and taken ashore for processing and disposal. (For interpretation of the figure legend, the reader is referred to the web version which is in color).

created around the MODU for safety reasons (Fig. 1C, see S1 for a schematic representation). The 3 well batch drilling was completed over 164-day period between 27 March and 7 September 2017.

The 42″ and 26″ sections (referred to as 'top hole' sections) were drilled as an open system without a riser (i.e., riserless), which meant that drill cuttings and drilling fluids were discharged directly from the wellbore to the seabed. This can create very localized piles of cuttings (IOGP, 2003). The remaining sections (referred to as bottom hole sections) were drilled 'closed' with a riser pipe in place (Fig. 2B), which means that the discharge of cuttings and drilling fluids was from the MODU and therefore there is a greater possibility for wider dispersal than discharging at the seabed (IOGP, 2016). Discharges were from the MODU from a 12.5″ diameter outlet at a depth of 23 m below the sea surface (see S2, S3). Water based drilling fluids (WBDFs, 'spud-mud' with a small volume of barite) were used for the 42″ and 26″ sections. The 17.5″ sections were drilled with two WBDF systems, a gel-polymer mud when passing through the upper geological formations (from ~300–1140 m) and a KCl-polymer mud used for the lower formations (1140–2300 m) (Fig. 2B). WBDF were discharged intermittently in batches when the fluid systems were changed (see also Melton et al. (2000)). For the 8.5″ sections a water-based reservoir drill-in fluid was used (Fig. 2B).

Non-aqueous drilling fluid (NADF, following the nomenclature of IOGP (2016)) was used for the 12.25″ sections (Fig. 2B), and all NADF was retained on the MODU and returned to the shore for recovery and recycling. Some residual NADF discharge would have occurred as mud still adhered to cuttings, but cuttings discharge was only permitted if the average oil content was <10% wt/wt (on dry cuttings) after passing the wet NADF cuttings through the cuttings dryer system. NADF may also enter the marine environment after washing mud pits which have previously contained NADF, although discharge was only allowed if with the oil by volume content of the washings was <1%. For further general information on typical solids control processes see IOGP (2016) (IOGP, 2021) and IOGP (2003).

Solids control equipment was used to separate cuttings from drilling fluids and cuttings were passed over a series of shale shakers (see images in S2) with 80 mesh (177 μm cut point) on the upper scalper deck and 170 mesh (88 μm cut point) on the lower deck. Material <88 μm was recirculated through the wellbore, and >88 μm discharged overboard as cuttings (see S2, S3). Decanting centrifuges were also used for the muds before reuse to reduce the drill solid (fines) content and maintain the rheological properties.

1.3. Drill cutting and drilling fluid quantification

Data on the drill cuttings and drilling fluid discharges were obtained from the proponent's and drilling contractor's end of well environmental discharge reports, daily mud reports, operational discharge logs, and daily drilling reports. This data was used to derive input parameters for the discharge trajectory and fate modelling and was supplemented with additional cuttings and mud sampling from the MODU and underneath the MODU using instruments mounted to an ROV (Oceaneering Ocean Magnum 126, S2, S3).

Instruments mounted to the ROV frame included a nephelometer (In Situ Marine Optics, Perth, Western Australia) and a conductivity-temperature-depth profiler (RBRConcerto, Ottawa, Canada). Water (plume) samples were also collected using 3 × 1.2 L ROV Niskin™ bottle (General Oceanics, Miami, Florida, US) mounted to the ROV frame (see images in S2, S3). At the end of the sampling the ROV was returned to the MODU platform and data from the instruments downloaded and the water samples decanted to 1 L plastic wide-mouth containers for subsequent analysis. The timing of the water sampling was recorded to the nearest second and all sampling was recorded by the ROV high definition cameras.

During the drilling of the 17.5″ section of the first well, 6 drill cuttings samples were collected at regular depth intervals through the different formations (LPA1 in Fig. 2F) from the scalper and lower deck of the shale shaker (Table 1, see images in S2). Soon afterwards, samples were collected from the discharge line access port after passing through the fine removal units (centrifuges) (S2). During the drilling of the 17.5″ section of LPA1, 10 L samples were also collected from the mud pits containing a WBDF gel-polymer mud and KCl-polymer mud. All samples were decanted into glass jars and a few mL of the antibacterial biocide benzalkorium chloride added before transport to the laboratory. Wet and dry bulk density was determined for the cuttings samples and gel-polymer and KCl-polymer muds. Particle size distributions (hereafter PSDs) of the drilling fluids (also termed muds) were measured using a

Table 1
Sampling activities during the drilling program (see Fig. 2 for the timing of activities).

Above water sampling on the MODU	
Wind speed and direction	Obtained from the Goodwyn Alpha Platform and from the North Rankin Complex A (converted to 10 m above ground) (Fig. 1A)
Cuttings	6 cuttings samples collected from the lower deck of the shale shaker at regular depth intervals through the different geological formations (Fig. 2F) of the 17.5″ section of the LPA1 well (S2).
Centrifuge	7 samples collected from the discharge line access port after passing through the fine removal units (centrifuges) shortly, after the cuttings sampling (above) (S2).
Drilling fluid	2 samples of used gel-polymer and KCl-polymer collected from the mud pits before discharge and 2 unused samples of gel-polymer and KCl-polymer provided by the drilling contractor.
Model input data	End of well environmental discharge reports, daily mud reports, operational discharge logs, and daily drilling reports.
ROV-based in situ sampling within 200 m of the drill centre	
Water	40+ plumes samples collected using Niskin™ bottles mounted to the ROV frame (S2 and S3).
Turbidity, temperature, and conductivity	Vertical and horizontal profiles measured using a nephelometer and conductivity-temperature-depth probe mounted to the ROV frame
Current speed and direction	Collected using an acoustic doppler current profiler (ADCP) mounted onto a sensor platform (S2) placed on the seabed (Fig. 1D)
Light measurements and depth	Underwater photosynthetically active radiation measured with an 8 wavelength multispectral sensor mounted on the instrument platform (S2).
Seabed	11 seabed samples collected using a sediment grab (S2) 50 m, 100 and 200 m along some of the 200 m transect lines emanating from the drill centre (see Fig. 6)
Ecological surveys	8 × 200 m transects recorded by downward facing high definition video camera mounted to the ROV before drilling (4–5 November 2016), during drilling (5–6 May 2017) and after drilling (26–27 August 2017) (results Figs. 10, 11, S7). High resolution images were captured at 6–7 m intervals
Ship-based sampling at Rankin Bank and Glomar Shoal > 2 km from the drill centre	
BRUVS	48 (Rankin Bank) and 24 (Glomar Shoal) stereo baited remote underwater video stations (BRUVS) deployed at least 250 m apart over the period 17–25 January 2017 (prior to the start of drilling) and subsequently from 11 to 21 December 2017 (results Fig. 12, S10).
Towed video (TowVid)	17 (Rankin Bank) and 10 (Glomar Shoal) ~1.5 km transect lines collected from 17 to 25 January 2017 (prior to the start of drilling) and subsequently from 11 to 21 December 2017 using a forward-pointing live-feed high definition video camera mounted to an aluminium sled. High-resolution still images were captured at 10 s intervals (~6–10 m spacing)
Seabed	17 (Rankin Bank) and 11 (Glomar Shoal) sediment samples collected by a Smith and MacIntyre Grab from 17 to 25 January 2017 (prior to the start of drilling) and subsequently from 11 to 21 December 2017.

laser in-situ scattering and transmissometry (LISST) 100× Type C (Sequoia, WA, US). Approximately 100 samples were examined and averaged per suspension and from the PSD the total volume concentration, mean and median particle diameter were determined. The optical model can be based on light scattering by spherical or random shapes. The spherical model was used with 90 μm silica beads used as an internal quality assurance and quality control procedure, but for the drilling muds the random shape kernel supplied by the instrument manufacturers was used.

The PSDs of the gel-polymer mud and KCl-polymer WBDFs sampled from the pit prior to discharge were also determined using the LISST. Back-scattered electron imaging and scanning electron microscopy and elemental analysis using Energy-dispersive X-ray spectroscopy (see S4 for methodology) was used to examine the two types of mud including new (unused) samples and used samples collected from the mud pits.

The settling times of cuttings and muds samples for the modelling and was determined in a settling tube with an internal balance which measures the mass of sediment settled over time (Kench and McLean, 1997). A 10–15 g sample was placed onto the top of a release mechanism above a 0.25 diameter, 2.5 m long cylinder. The cylinder had a mass with a plate suspended below it at a depth of 1.875 m below the release mechanism. When the release mechanism is opened the sediment is dropped into the dispersant and a limit switch activates which begins recording time and weight of sediment deposited on the pan. The results were corrected to the settling rate at a water temperature of 20 °C and settling velocities are converted to grain-size distributions using methods described in Gibbs et al. (1971).

1.4. In situ sampling

To facilitate navigation around the wells, 8 georeferenced sonar contact buoys were temporarily installed 200 m away from drill centre on cardinal and intercardinal compass points (Fig. 1D). Current speed and direction during the drilling of most of the 17.5″ sections was measured using a RDI 300 kHz Workhorse sentinel acoustic doppler current profiler (ADCP) mounted onto a sensor platform near (S2, Table 1). The sensor platform was deployed on the seabed 200 m NW of the drill centre near one of the sonar marker buoys (Fig. 1D) with the ADCP acoustic transducer positioned 2.0 m above seabed. Additional instruments on the platform included an 8 wavelength (MS8) multi-spectral photosynthetically active radiation sensor and a DL3 three-channel data logger (In Situ Marine Optics, Perth, Australia). Tidal information over the drilling campaign was derived from the depth sensor in DL3 three-channel data logger.

On several occasions during drilling of the 17.5″ sections and before and after the mud pit and cuttings discharges, a series of vertical and horizontal profiles were conducted by the ROV underneath the MODU. Measurements were made of turbidity and temperature using instruments mounted to upper frame of the ROV frame and water (plume) samples collected using Niskin bottles mounted to the front of the ROV (see images in S2, S3). These were triggered automatically from the MODU using an actuator (S2). Once returned to the MODU the samples were shaken to resuspend settled sediment and then turbidity measured (as nephelometric turbidity units, NTU) and total suspended solids (TSS) determined gravimetrically by filtering the samples onto Whatman 47 mm GF/F filters with ~100 mL of distilled water used to rinse the container, filter funnel and filter pads of salts. The filters were then dried overnight in an oven at 65 °C and weighed to the nearest 0.0001 g. In addition, 6 of the samples with TSS levels >200 mg L^{-1} were diluted (25% plume sample to 75% filtered seawater) and the turbidity and TSS determined, and the process repeated 5 more times. The mean NTU was used to generate the relationship between turbidity (NTU) and TSS (mg L^{-1}).

1.5. Seabed sediment sampling

On completion of the 17.5″ sections, surficial seabed sediment samples were collected by the ROV around the wells 50 m, 100 m or 200 m along the transect lines (see Fig. 1D for sampling locations, Table 1) using a powder coated, steel, cylindrical (50 cm × 12 cm internal diameter) sediment grab (S2). The grab was moved by the ROV manipulator arm over the seabed surface to capture sediments to a depth of ~5 cm and then closed using the other manipulator arm by rotating an attached circular end cap over the cylinder mouth. Sediments were subsampled from the grab and placed in 100 mL glass jars and refrigerated for subsequent chemical analyses for trace metal and particle size analysis (see below).

Surficial sediment samples were also collected from Rankin (n = 17) and Glomar (n = 11) (see Fig. 1B and C for sampling locations) using a Smith-McIntyre grab operated from the Australian Institute of Marine Science's (AIMS) oceanographic research ship *RV Solander* before (January 2017) and after (December 2017) the drilling campaign. Sediments were subsampled from the grab and placed in 100 mL glass jars and refrigerated for subsequent chemical analyses for trace metals analysis of Sb, As, Ba, Be, Cd, Co, Cr, Cu, Pb, Mn, Ni, Zn (using Inductively Coupled Plasma Optical Emission Spectrometry (ICP-OES) using a Varian Vista Pro ICP-OES), and Hg (by cold vapour AAS using a CETAC auto analyser). All analyses were conducted at the ChemCentre (Perth, a NATA Accredited facility). Wet sieving and laser diffraction techniques (ISO 13320:2009) were used for particle size analysis of all seabed sediment sample.

1.6. Plume modelling

Near-field modelling was conducted with CORMIX (Cornell Mixing Zone Expert System, Version 11.0GTD, DHYDRO Version 11.0.0.0 April 2018) (Jirka, 2006) which also includes a jet integral model to predict the jet trajectory and dilution characteristics and far-field modelling was conducted using Delft3D (Delft Hydraulics, Deltares (2011)). The bathymetric dataset used for the model domain development was provided by Woodside from a series of surveys by Fugro Survey Pty Ltd. over water depth ranging from 19 to 128.3 m using a Reson Seabat 7101 multibeam echo sounder.

A nested grid system was developed composed of multiple sectors with different grid sizes in a 1:3 ratio hence levels of spatial resolution. Considering that the numerical model would be forced by tides and wind only, this technique allows isolation of the region of interest from the boundary effects from the outer area. The outer grid had a horizontal spatial resolution of 450 m, the intermediary grid 150 m and the finer grid resolution 50 m, centred on the drill centre (see S5). All grids had 8 vertical σ-layers, equally distributed over the vertical axis and a vertical resolution of each layer was ~10 m. The outer grid was forced by tides (one way) and the coupling among the inner grids (white and blue ones) had a dynamic interaction (two ways or bi-directional) through their boundaries, thus the outer grid received information from the forcing files through the green lines and interacts with the intermediary grids exchanging information on both ways through the red lines boundaries (S5).

The space varying tidal component data were extracted using the Tidal Model Driver (TMD) to provide the open-ocean boundary conditions to the Delft3D model. Tidal Model Driver is a Matlab data processing package based on the TPXO7.2 tidal model (available at http://volkov.oce.orst.edu/tides/TPXO7.2.html), which assimilates various satellite altimetric datasets (e.g. Topex Poseidon, Topex Tandem, ERS, GFO), as well as in-situ observations (see Egbert and Erofeeva (2002)). The diurnal tidal components applied to the open boundary were K1, O1, P1 and Q1, and semi-diurnal tidal components were M2, S2, N2 and K2. Additionally, long-period components Mf (lunisolar fortnightly, the effect of departure from a sinusoidal declinational motion), Mm (lunar monthly, the effect of irregularities in the Moon's rate of change of

distance and speed in orbit) were used. Wind speed and direction records (converted to 10 m above ground) were obtained from the Goodwyn Alpha Platform and from the North Rankin Complex A (Fig. 1A, Table 1).

The spatial and temporal distribution of sediment concentration at the end of the near-field were prescribed and assimilated by the far-field model (Morelissen et al., 2013; Niu and Lee, 2013). The coupling between the near and far-field models was performed by releasing the sediments in the cells of the Delft3D grid occupied by the plume of sediments at the end of the near-field. The three-dimensional spatial arrangement of these cells was determined by the Cormix, which provided the displacement x, y, z, in addition to the thickness and width of the plume of sediment and the respective dilution as a function of the distance from the discharge point. To assess the dilution and long-range transport, TSS concentrations as well as settlement of the discharges and resulting sediment thickness, a number of 'observation points' were added to the model domain at 200–1000 m away for each cardinal and intercardinal compass points.

1.7. Ecological surveys

1.7.1. Video surveys (via ROV) around the drill centre

Ecological surveys of the epibenthos were conducted around the wells along the eight × 200 m environmental survey lines (Fig. 1D) before drilling (4–5 November 2016), during drilling (5–6 May 2017) and after drilling (26–27 August 2017) (Fig. 2C) using forward and downward facing high-definition cameras mounted to the ROV. During the surveys, the ROV began at the drill centre and moved along the survey lines to the sonar marker buoys, navigating at a speed of ~0.15 m s^{-1} and distance of ~50–100 cm above the seabed. Video was captured with forward facing (35–45° from horizontal) and downward facing high definition cameras (HDTV, 1920 × 1080 @ 25 fps). ROV video lights were used during the surveys and still images were captured from the video at equal distances along each transect (approximately ~6.5 m apart). Although the images were not georeferenced, positions were estimated from the georeferenced sonar marker buoys at the ends of each transect.

1.7.2. Towed video surveys at Rankin and Glomar

Ecological surveys also investigated the distribution and abundance of epibenthic habitats across Rankin Bank (n = 17 sites) and at a reference site Glomar Shoal (n = 10 sites) 125 km ENE of Rankin Bank (Fig. 1A). Although Glomar is distantly located from Rankin Bank it was the only possible reference site, enabling broad scale comparisons of, for example, Ba concentrations, and contextualization of changes in epibenthic groups (for example seasonal changes in algae).

Surveys were conducted from the AIMS ship *RV Solander* using a towed video system comprised of a lightweight tow body with forward-pointing live-feed video and a downward-pointing camera, light sources, and an ultra-short baseline system for geo-locating the towed body on the seabed. Surveys were undertaken along the ~1.5 km transect lines from 17 to 25 January 2017 (prior to the start of drilling) and subsequently from 11 to 21 December 2017 (following the cessation of drilling activities). Transects were chosen to include sites that had been previously sampled by AIMS in 2013 and 2014 to provide longer-term perspective of natural variability in these communities, and in particular to include areas of known coral and filter feeder communities that might be most susceptible to any drilling activities. Transects were surveyed at 1.5 knots, usually beginning shallow and progressing into deep water. Live-feed from the video and a variable speed winch allowed observers on the vessel to maintain the tow body 30–50 cm above the seafloor. High-resolution still images from the downward facing camera (with a field of view between ~0.1 and 0.25 m^2) were captured at 10 s intervals (~6–10 m spacing).

Still images from ROV and towed video cameras were characterised using a point-intercept method, whereby the benthos underlying 20 regularly spaced points (ROV-surveys) and 5 points (towed video surveys) per image were identified to the highest taxonomic classification or morphotype using the AIMS Reefmon software (Jonker et al., 2008). To compare the composition of epibenthic communities before and after drilling, percentage cover of the benthos was standardised to 100% cover per image for both ROV and towed video surveys. For towed video surveys, benthic cover was further summarised by location, survey time, transect and depth. The latter was split as shallow (<40 m) and deep (≥40 m), reflecting a known transition in benthic communities (Abdul Wahab et al., 2018). Transects that spanned shallow and deep areas were only included in the analyses if sample size comprised at least 15 images at each depth.

Multivariate analyses in PRIMER 7 (Clarke and Gorley, 2015) with PERMANOVA+ (Anderson et al., 2008) were used to determine whether changes observed in pre- and post-drilling towed video surveys at Rankin Bank were within or greater than the range of variability observed at Glomar Shoal. A subset of the fine-scale biotic categories (excluding algal groups) was selected for these analyses with data square root transformed and Bray-Curtis similarity matrices constructed. Hierarchical cluster analysis was carried out by pairwise comparisons using group average clustering and a similarity profile routine (SIMPROF, Clarke et al. (2008)) for 999 permutations at a significance level of 5% used to determine significant groupings. Non-metric multidimensional scaling (nMDS) ordinations were overlayed with SIMPROF groups to highlight similarities among transects. Differences among groups were tested using permutational multivariate analysis of variance (PERMANOVA) with fixed factors for location, time and depth and a random factor of transect nested within location.

1.7.3. Baited remote underwater video stations (BRUVS)

Demersal fish communities were surveyed using stereo baited remote underwater video stations (BRUVS) (Cappo et al., 2007; Harvey et al., 2002; Whitmarsh et al., 2017) to assess broad-scale trends in richness, abundance and fish community structure at Rankin Bank and Glomar Shoal before and after drilling activity (Table 1). A total of 48 BRUVS were deployed at Rankin Bank and 24 BRUVS at Glomar Shoal at each time period (144 deployed; Fig. 1B, C), with 141 videos having unobstructed field of view and being suitable for analysis.

The BRUVS were baited with 1 kg of crushed pilchards (*Sardinops sagax*), suspended in a plastic-coated wire mesh bag 1.2 m in front of the cameras and deployed for 1 h with a minimum distance of 250 m between deployments to avoid potential overlap of bait plumes and the movement of fish between BRUVS. The bait type used and the bait bag location with respect to the camera, as well as the bait replacement frequency, camera resolution and image capture rate, and deployment times of day are all consistent with standardisation guide of Langlois et al. (2020). The BRUVS were positioned to overlap as much as possible with towed video transects at each site (Fig. 1B, C) and a minimum distance between BRUVS of 250 m is consistent with Langlois et al. (2018). The possibility of large bodied mobile fish moving between BRUVS during the deployments is acknowledged, but the likelihood of this was minimised by rapid deployment of the BRUVS suite so soaking time overlapped, reducing the probability of fish leaving one baited system for another (Birt et al., 2019).

BRUVS videos were analysed to determine species diversity, relative abundance (as MaxN) (Cappo et al., 2004; Priede et al., 1994; Schobernd et al., 2014; Willis and Babcock, 2000) and community structure. Unidentified taxa (identified only to genus) and fishes that were difficult to identify on video footage at depth, and therefore were subject to variability in identification by readers, were grouped for statistical analysis. Seabed composition was derived from the BRUVS field of view as a proportion of biotic cover of filter-feeders, encrusting organisms, hard coral, bare substrate, and abiotic cover of calcareous reef and gravel/rubble/sand habitat. Spatial predictors included depth (categorised as shallow <40 m, deep >40 m), site position (latitude, longitude), and topographic data at BRUVS sites derived from multibeam sonar (Abdul

Wahab et al., 2018) including aspect (azimuthal direction of the steepest slope), slope (average change in elevation/distance), curvature (combined index of concavity/convexity parallel and perpendicular to the slope) and local relief (rng50; at kernel pixel radius 50). Pre- and post-drilling Barium concentrations derived from nearby sites were included for each BRUVS sample at Rankin Bank, to identify any trend in Barium levels as a result of drilling activity.

To test the effects of drilling (pre- and post-drilling surveys) compared to spatial, habitat and environmental predictors as drivers of fish community structure, fish genera present on at least 5% of samples were included in distance-based redundancy analyses (dbRDA) for each shoal. The distance matrix (dissimilarities) was calculated on the transformed abundance (4th root MaxN) data for genera using the site-standardised (Manhattan distance) extended dissimilarity (xdiss() in library mvpart; De'Ath, 2002). The eigenvalues obtained in the PCoA were used with the capscale function to perform the ordination (dbRDA) via the vegan package (Oksanen et al., 2018). Capscale uses non-Euclidean dissimilarity indices yet remains strictly linear and metric. The variation accounted for by each axis, was provided by permutation tests which assessed significance of each spatial and environmental predictor via pseudo-F values. Use of the envfit() function (library vegan) identified the direction of abundance vectors for fish genera (in the k-dimensional ordination space) that had maximal correlation with predicting relationships with spatial, habitat and environmental predictors. Models were conducted for each shoal, and also for a subset of 13 BRUVS sites closest to the well centre (transects 1–5) at Rankin Bank. All analyses were conducted in the R environment (R Core Team, 2017).

2. Results

2.1. Drill cuttings and drilling fluids discharges quantification

Drilling occurred over 496 h (on 38 separate days) over the campaign, and the distance drilled per day varied from 58.2 m to 1024 m (Fig. 2D). The total volume of cuttings generated from the 3 wells was 1543 m^3 (based on the diameter and length of each of the sections) or 4012 t (based on an average bulk density of 2600 kg m^{-3}). Overall, 19.5% of the total cuttings (301 m^3 or 783 t) were discharged directly to the seabed during the drilling of the 42″ and 26″ sections (Table 2). The largest mass of cuttings discharged from the MODU was associated with the 17.5″ sections (2540 t and 63% of the total) which was 4× the amount discharged from the 12.25″ sections. Barite use was primarily associated with the 17.5″ and 12.25″ sections (Fig. 2E) and 150 t was released to the environment as mud adhering to cuttings, and with operational discharges (17.5″ sections only). A total of 287 t of bentonite was used to mix the gel-polymer mud and was also released to the environment as sweeps, as mud adhered to cuttings and operationally discharged on emptying and cleaning the mud pits.

Cuttings discharges rates were calculated from the total mass of cuttings produced divided by the hours of drilling assuming the drilling was continuous (Pivel et al., 2009) and varied by over an order of magnitude between sections, averaging ~8–9.3 kg s^{-1} for the riserless sections, 2.9 kg s^{-1} for the 17.5″ sections and 0.8 kg s^{-1} for the 12.25″ sections (Table 2).

Over the batch (three well) drilling campaign 12,932 m^3 of brines, WBDFs or NADFs (as mud adhering to cuttings) and completion fluids were released during the campaign. Of this, 25 m^3 was lost to the atmosphere through evaporation, 962 m^3 was lost below the seabed (by permeation of the porous formations), and 6 m^3 of muds was recorded as lost from deck washing (which was collected in tanks and taken ashore for processing and disposal) (Table 3, Fig. 2).

Total WBDFs discharged to the seabed (during the initial drilling of the riserless top-hole sections) was 1795 m^3, and fluids lost from the MODU as mud adhered to cuttings after processing through the shale shakers was 444 m^3, of which 90% was from the drilling of WBDF sections (Table 3, Fig. 2). Volume losses after the solids control processes (centrifuges) and dryers (12.25″ sections only) was 428 m^3, similar to losses by mud adhered to cuttings.

Overall, the greatest loss of fluids from the MODU, as WBDF and brines was from planned drilling fluid discharges (9205 m^3), noting that NADFs were retained and returned to the shore for recovery and recycling. (The discharge of 305 m^3 from the 12.25″ sections (see Fig. 2B) was of previously stored WBDF which was discharged to create storage room.) Muds and brines were not separated in the mud logging data recordings but for the 8.5″ sections where WBDFs were used, the discharges were primarily brines with very low solids content. Additional seawater discharges from the MODU which may have contained low level traces of solids were associated with washing the mud pits with seawater and amounted to 8988 m^3 (Fig. 2B).

2.2. Particle size distributions and settling velocity

Some silt and clay sized particles were found in samples collected from the shakers in the first two sampling depths (340 m and 680 m) of the 17.5″ section; however, overall, there was no consistent pattern of changes in grain size or density with drilling depth. Overall >95% of the cuttings were >1 mm (very coarse sand) and 63% >2 mm (fine pebble size), with an average grain size of 1775 ± 179 μm, a wet bulk density of 1740 ± 0.05 kg m^{-3} and grain density of 2300 kg m^{-3} (Table 4). The mud samples collected from the mud pits just before discharge were ~90% silt sized (<62.5 μm) with a mean diameter of 12 μm (gel-polymer) and 33 μm (KCl-polymer) and wet bulk densities of 1300 kg m^{-3}. TSS levels in the gel-polymer mud (257 g L^{-1}) and KCl-polymer mud (245 g L^{-1}) sampled just before discharge were very similar (Table 4). TSS levels in the centrifuge waste stream averaged 46 ± 8 g L^{-1} ($\bar{x}$ ± 95% confidence intervals, n = 7, range 17–78 g L^{-1}, Table 4).

The new (unused) KCl-polymer contained many rhomboidal and rectangular particles with the elemental analysis indicating an association of these particles with Ba and/or K and Cl (S4). The gel-polymer mud had extensive planar, flat lying sheets of material with the elemental analysis indicating an association with Si, Al and Fe indicating they were sodium bentonite, an aluminium phyllosilicate smectite clay composed mostly of montmorillonite with K and Fe as common substitutes (S4). Microscopical analysis of the used formulations showed

Table 2
Drill cuttings generation and chemical discharges. Summary statistics of the estimated volume and mass of cuttings discharges for all three wells (with mass based on a density of 2600 kg m^{-3}) and discharge rates (kg s^{-1}). The drilling times for the 8.5″ sections were not available, but the cuttings generated were only 1% of the total and a discharge rate assumed to be the same as the 12.25″ sections.

	Riserless		Riser in place			Sum
Section	42″	26″	17.5″	12.25″	8.5″	
Length (m)	169	439	6296	3230	510	10,644
Volume (m^3)	151	150	977	246	19	1543
Mass (t)	393	391	2540	640	49	4011
Mass (%)	9.80%	9.74%	63.33%	15.92%	1.21%	100%
Drilling time (h)	12	15	244	217	17	503
Cuttings discharge rate (kg s^{-1})	9.3	8.0	2.9	0.8	0.8	

Table 3
Losses of brines, WBDF and NADF and RDF during the batch drilling campaign. Values are the discharge volumes (m^3) for all 3 wells. Also included is completion (compl.) fluid discharges and mud-pit wash volumes which are released through the discharge line under the MODU, subsea control fluids from BOP testing, cement discharges and treated water.

	Section:	42″	26″	17.5″	12.25″	8.5″	Compl.	Sum
		WBDF (spud mud)		WBDF	NADF	RDF		
Drilling fluid loss		Riserless		Riser in place				
Evaporation	Air	0	0	0	25	0	0	25
Formations	Below seabed	0	0	406	111	22	420	960
Mud Vac waste[a]	Ashore	0	0	0	6	0	0	6
Cuttings dryer (NADF)	Sea	0	0	0	172	0	0	172
Centrifuge	Sea	0	0	193	63	0	0	256
Shale shakers (WBDF)	Sea	0	0	398	0	38	0	436
Planned discharges	Sea	728	1067	2693	305[b]	4412	1864	11,069
Sum		728	1067	3690	683	4472	2284	12,924

[a] Refers to muds lost to the MODU deck when changing drill strings which is directed to storage tanks using a vacuum or a draining system and then taken ashore for processing and disposal.
[b] Previously stored WBDF which was discharged during the drilling of the 12.2″ sections.

Table 4
Drilling cuttings and drilling fluid particle size analysis. Mean particle size distribution (±95% confidence intervals) and density of cuttings samples collected from the shale shakers at ~300 m intervals down the LPA1 well sampled between 340 and 2176 m below sea level, and for the drilling fluids in samples from the mud pits just prior to discharge. Particle size distribution was simplified to 5 and 9 sediment classes for the cuttings and discharge modelling respectively.

Distribution	Phi	μm	Drill cuttings			Drilling fluids				
			Sediment class	Mean	95% CI	Sediment class	Gel-mud	KCl mud	Mean	95 CI
Fine pebbles	−2	>4000	1	0.6	0.5		0.9	0.0	0.5	0.5
Very fine pebbles	−1	>2000		62.4	12.2		0.0	0.0	0.0	0.0
Very coarse sand	0	>1000	2	33.4	11.2		0.0	0.0	0.0	0.0
Coarse sand	1	>500	3	1.8	0.4	1	0.0	1.2	0.6	0.6
Medium sand	2	>250	4	0.6	0.2	2	0.0	1.4	0.7	0.7
Fine sand	3	>125		0.2	0.1	3	0.0	8.1	4.1	4.1
Very fine sand	4	>62.5		0.1	0.1	4	0.0	15.9	8.0	8.0
Coarse silt	5	>31.3	5	0.1	0.1	5	0.0	18.4	9.2	9.2
Medium silt	6	>15.6		0.2	0.2	6	0.0	15.5	7.8	7.8
Fine silt	7	>7.81		0.2	0.2	7	3.1	13.4	8.3	5.2
Very fine silt	8	>3.91		0.3	0.3	8	61.7	9.2	35.5	26.3
Clay	9	>1.95		0.0	0.0	9	34.3	16.9	25.6	8.7
Phi				−0.78	0.16		6.39	4.91	5.65	0.74
Mean μm				1775	179		12	33	23	11
Wet bulk density (g cm^{-3})				1.74	0.05		1.30	1.30	1.30	0.00
Grain density (g cm^{-3})				2.30	0.03		–	–	–	–
TSS (g L^{-1})				45	8		245	257	251	6

loss of Ba, and the sheet like structures were less pronounced, and both mud types contained numerous Ca particles from the calcareous sedimentary rocks in the geological formations (S4). Based on the microscopical analyses a random as opposed to spherical kernel matrix (supplied by the LISST manufacturers) was used for the PSD analyses (Fig. 3A).

The used WBDF samples taken from the pits before discharge and plume samples collected after discharge had very clear peak particle size distributions in 15–50 μm range or medium and coarse silt (see Fig. 4A for representative samples and S6 for all samples). The samples of used KCl- and gel-polymer WBDFs (collected from the mud pits prior to discharge) and plume samples of used KCl- and gel-polymer collected under the MODU by the ROV were used to establish the linear relationship between NTU and TSS shown in Fig. 4B (where TSS = 1.45 × NTU, R^2 0.96). This relationship was applied to the turbidity data collected by the ROV-mounted nephelometer (see Fig. 4) to derive a TSS proxy or surrogate measurements for validation of the model outputs.

PSDs in seabed sediment samples collected around the drill centre were complex with a tri-modal size distribution and distinct populations of fine and very fine silt (<10 μm diameter), silts and fine sands (see Fig. 3C for seabed PSDs on transect line 7 at 50 m, 100 m and 200 m from the drill centre and S6 for all samples collected). The samples are likely to have contained native sediments from the seabed, fragments of the various geological formations (crushed formation rock) brought up as cuttings, and different types of WBDFs containing fine suspensions of barite and bentonite clay particles from the mud pit discharges. The finest size distribution was in the 50 m sample collected on the western transect which showed a bi-modal distribution peaking at 3 μm diameter (clay-sized range) and 50 μm (Fig. 3C) and very low numbers of particles >200 μm diameter. The sample had the highest Ba concentrations (see and Fig. 5A, B).

Particle diameters of the cuttings and mud samples spanned over 3 orders of magnitude (2 to >2000 μm) (Table 4) and the settling velocity spanned over 5 orders of magnitude (10^{-6} to $>10^{-1}$ m s^{-1}) (Fig. 3D). These settling velocities were used for the plume trajectory modelling (see below).

2.3. Plume TSS concentrations

Mud pit discharges exited the discharge outlet as a jet of material in a distinctive cloud-like plume descending rapidly to the seabed and growing in diameter with increasing depth (Fig. 4, see images in S2, S3). The base of the plumes was followed by the ROV which was manoeuvred into and out of the descending plume continuously recording turbidity and temperature (see images in S3). Nephelometrically-derived TSS concentrations were <0.5 mg L^{-1} in clear water outside the plumes, but inside the plumes, and close to the discharge outlet, TSS levels exceeded the maximum range of the nephelometer (600 mg L^{-1}). TSS levels

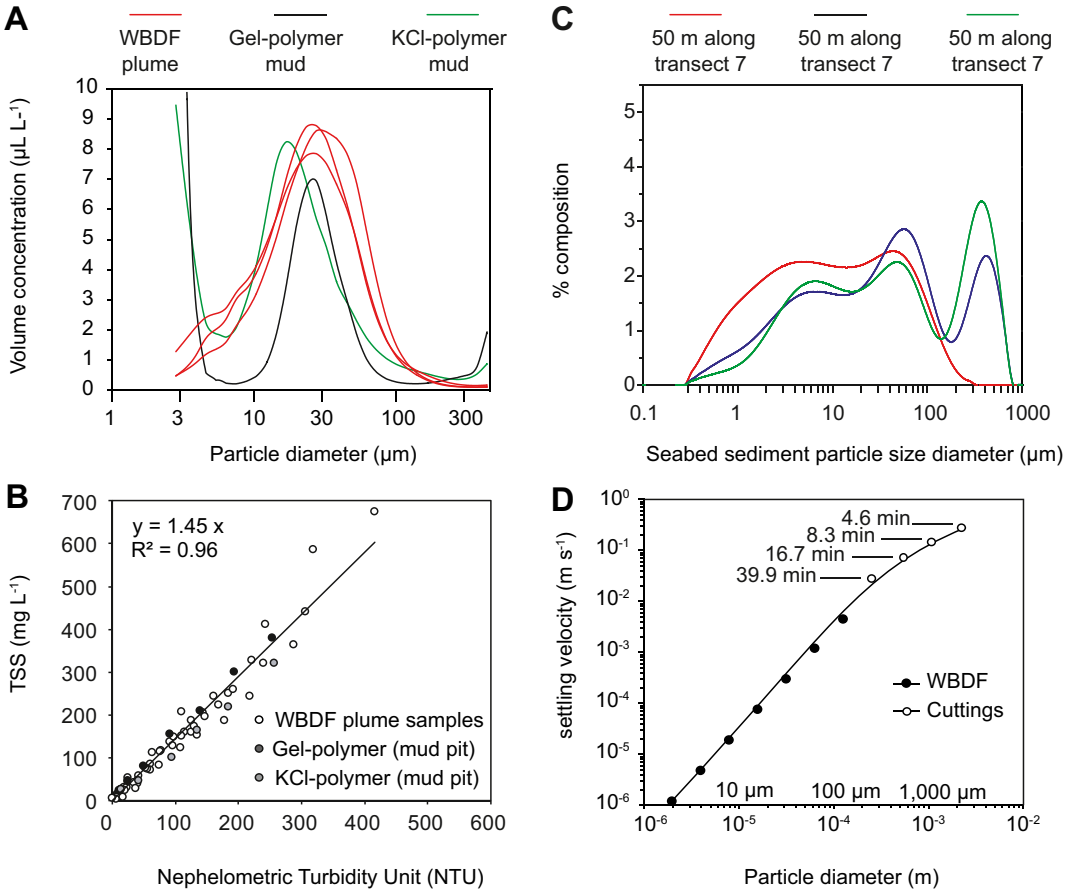

Fig. 3. (A) Particle size distributions (PSD) of some of the plume samples collected by the ROV under the MODU, and Gel-Polymer and KCl polymer mud collected from the mud pits prior to discharge (see S6 for all samples), (B) relationship between nephelometric turbidity units (NTU) and TSS (mg L^{-1}) from water samples collected in the discharge plumes under the MODU and WBDFs sampled from the mud pits prior to discharge, (C) PSDs of some of the seabed samples (see text) collected by the ROV under the drilling rig (see S6 for all samples), (D) particle diameter dependent variation in fall velocity (m s^{-1}) for the drilling fluids and cuttings. The values above the cuttings settling velocities are estimates of the time (minutes) for cuttings to fall from the outfall to the seabed under still conditions based on the fall velocity. (For interpretation of the figure legend, the reader is referred to the web version which is in color).

exceeding this maximum range were encountered at depths of up to ~35 m below sea level (Fig. 4D). In the 35–55 m depth range, TSS levels of up 500–600 mg L^{-1} were recorded and from 55 m to the seabed TSS levels were up to 200 mg L^{-1} were recorded (Fig. 4D). No turbidity was recorded on entering plumes made up of cuttings only.

Temperatures recorded by the ROV-mounted CTD showed clear water column stratification with 3 distinct layers with different water temperatures (°) and density (kg m^{-3}) (Fig. 4D inset figure). This stratification was incorporated into the near-field modelling (see below and Rye et al. (2006)). The temperature of plumes exiting the outlet was only ~0.1 °C above ambient seawater at −25 m depth (data not shown).

2.4. Seabed sampling (chemical analyses)

There was some localized enrichment of chromium in the sediment samples collected by the ROV within 200 m of the drill centre, but all values were well below Australian sediment quality guideline values (SQGVs) (Simpson et al., 2013) (S7). However, barium concentrations were highly elevated around the wells with a mean value 749.1 ± 248.6 mg kg^{-1} ($\bar{x}$ ± 95 confidence intervals, n = 11) which was ~60× higher than at the reference site (Glomar, 11–12 mg kg^{-1}). The highest barium concentration (3000 mg kg^{-1}) was recorded at the single 50 m sampling location (Fig. 1D), which also had the finest PSDs (D_{50} of 10.4 µm) and was 260× higher than the mean at the reference sites. Barium concentrations at the ends of transect lines (200 m from the drill centre) all exceed 130 mg kg^{-1} (~10× greater than the reference samples). Sediment samples collected just outside the 2000 m exclusion zone were 40–60 mg kg^{-1} (Fig. 5B) compared to values of 10–20 mg kg^{-1}across Rankin Bank.

2.5. Metocean conditions and plume modelling

During the drilling of the 17.5″ section there were both neap and spring tides with a tidal range of 3.1 m and water temperatures at the seabed ranged ~1.6 °C from 26.5–28.1 °C (Fig. 6A). PAR levels (at 78 m) showed clear diel light cycles, but noon irradiances were very low, ranging from only 1–6 µmol quanta m^{-2} s^{-1} (Fig. 6A), and the daily light integral (sum of the per second quantum flux measurements over the day) was <0.01 mol quanta m^{-2} day^{-1}. Winds came from the ESE through to SSE (40–45%) with a median of 2.5 m s^{-1}, although there were several instances when wind speeds exceeded 8 m s^{-1} (Fig. 6B).

Currents measured by the ADCP over the deployment period were slowest 0.15–0.2 m s^{-1} near the seabed and increased consistently up the water column to 0.8 m s^{-1} in the near surface layers (Fig. 6C–F). Current roses showed a higher percentage of WNW currents in the lower third of the water column, NW currents in the middle third and NNW in the upper third of the water column (Fig. 6G).

Since all the field work, including fluid and cuttings and plume sampling, and all metocean measurements were made during the drilling of the 17.5″ sections of the 3 wells where the highest volume of the cuttings and muds were discharged, the focus of the modelling study was the 17.5″ sections (see Discussion). Discharge scenarios were developed

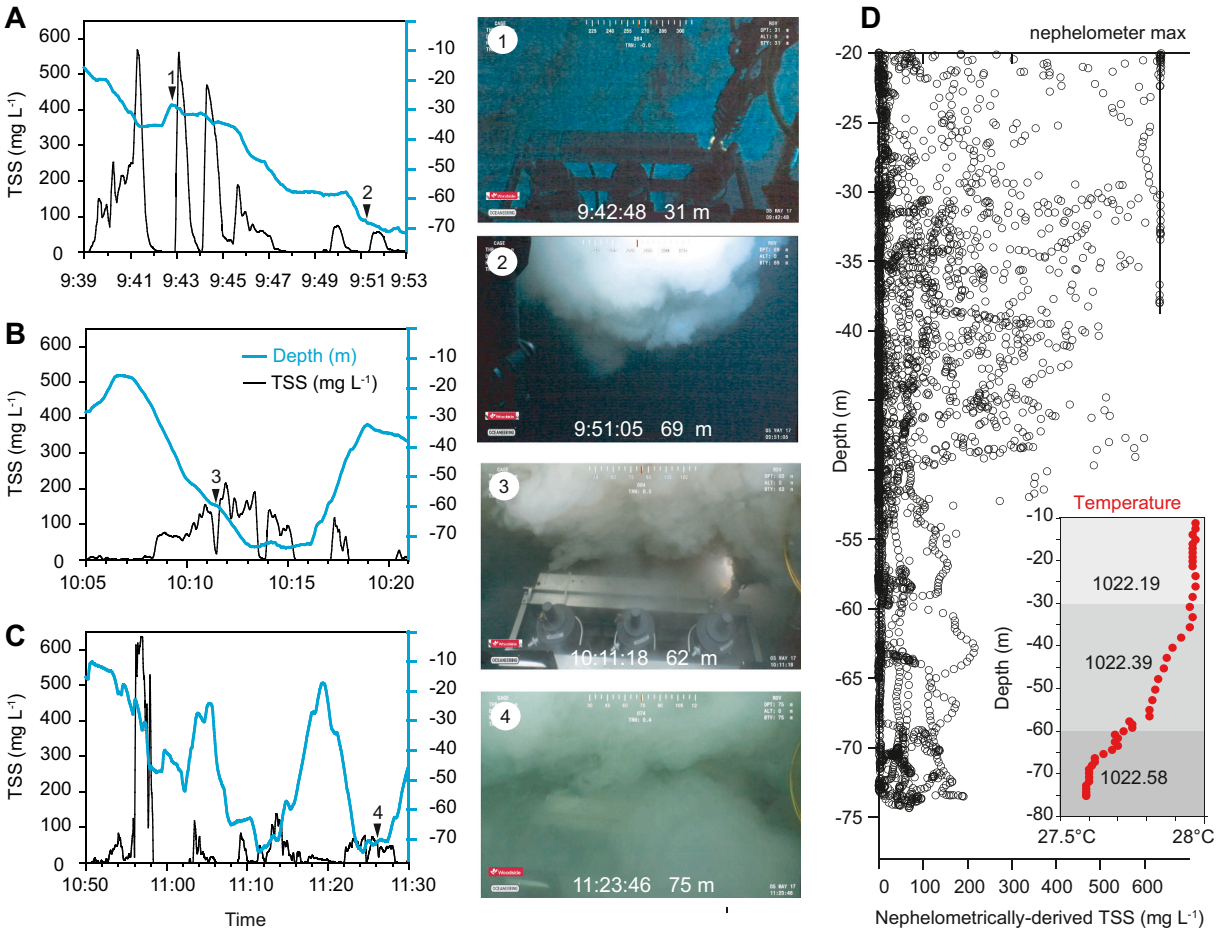

Fig. 4. (A–D) Representative nephelometry-derived TSS levels (mg L^{-1}) and depth (m) (secondary y-axis) profiles under the MODU after the discharge of the mud pits during the drilling of the 17.5″ section. Numbers 1–4 in the figures A–C correspond to the photographs taken by HDTV camera mounted on the ROV just about to enter plumes at water depths ranging from 31 to 75 m. (D) Vertical profiles of nephelometry-derived TSS levels and depth (m) or all plume sampling during the drilling of the 17.5″ section, and temperature (°C) for 1 vertical profile and specific density of the water column (kg m^{-3}). (For interpretation of the figure legend, the reader is referred to the web version which is in color).

to recreate events through the drilling campaign with some assumptions, generalizations and simplifications.

The total cuttings mass (kg) and production rates (kg s^{-1}) from Table 2 were used and although cuttings discharges occurred on 13 days (Fig. 2D), ranging from 4.5–24 h each day (totalling 235 h for all 3 wells), the cuttings discharges were simplified to 4 days of drilling for each well, with discharges occurring at a rate of 3 kg s^{-1} continuously over 20 h per day starting at midnight (i.e. ~1.5 tidal cycles each day). The PSDs and settling velocities of the cutting samples (collected along the length of the 17.5″ section of first well) were averaged and used for all wells. The cuttings contained some drilling fluids still attached to the particles after going through the solid control equipment (i.e., fluid adherence) and are represented by the small fraction of PSDs <62.5 μm in Table 4.

By far the majority of the drilling fluids lost to the marine environment from the 17.5″ sections were from the mud pit discharges (~95%) compared to losses after the solid control equipment (i.e. centrifuges in Table 3) and formation losses which were not considered as they are not relevant from an environmental perspective. For each 17.5″ section a gel-polymer mud was used when passing through the upper geological formations of the 17.5″ section and then KCl-polymer used for the lower formations (Fig. 2A, F). The muds were discharged after use, resulting in 6 major mud discharge sequences (numbered in Fig. 2B). The last event was the largest and involved the discharge of 667 m^3 (or >4000 barrels) to make storage room available for NADFs which were used on the subsequent 12.25″ sections.

The patterns of discharges that made up the 6 main discharge sequences were examined in closer detail from the operational discharge logs, and each was made up of multiple smaller discharges which averaged ~15 min long with a ~15-minute interval between. Discharges were not made on slack water (half an hour either side of high and low tide) and taking this information into consideration, and averaging across the 3 wells, the mud pit discharge modelling scenario was made up of 6 main discharge sequences, with each sequence composed of 6 smaller events each of 444 barrels and each lasting 15 min with a 15-minute interval between discharges. The drilling mud discharge rate was ~19.6 kg s^{-1} assuming 250 g L^{-1} (Table 4) or nearly 6.5× more than the cuttings discharge rate for the 17.5″ sections (Table 2). For the modelling, 2 scenarios were run with the 6 smaller discharge sequences starting 0.5 h after low tide or 0.5 h after high tide on each day that discharges occurred (Fig. 2B) using the locally specific hydrometeorological data on that day (Fig. 6).

2.6. Cuttings discharge modelling

The coarse cuttings (95% >1 mm) discharged from the 17.5″ sections of all 3 wells were modelled over 12 days and for each day occurred over a 20-hour period (or 1.5 tidal cycles) (Table 5). The simulated map of total cuttings accumulation created a roughly circular deposition field with a slight preferential movement to the west. There was a strong

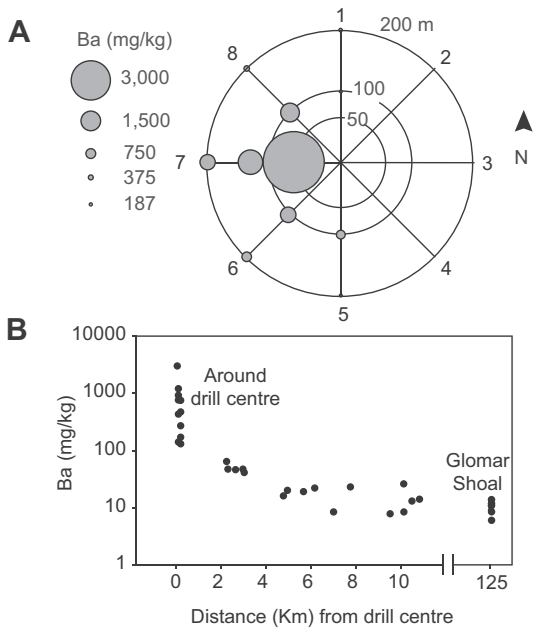

Fig. 5. (A) Polar plot showing Ba sediment concentrations (mg kg^{-1}) around the drill centre after drilling along the 200 m transect lines (B) Ba sediment concentrations (mg kg^{-1}) after drilling activities ordered by increasing distance from the drill centre taken near the towed video transects (see Fig. 1C).

gradient from >2 kg m^{-2} around the drill centre decreasing to up to 0.5 kg m^{-2} at 200 m (Fig. 7A). At the drill centre there was a proportionally greater build-up for the second cuttings discharge sequence (Fig. 7B), which occurred during neap tides (Fig. 6A) with lower current speeds (Fig. 6E). At the point 200 m W of the drill centre, there was a proportionally greater build up during the third sequence which occurred during spring tides where there was greater hydrodynamic transport of cuttings away from the drill centre (Fig. 7B).

For the drilling fluids, the CORMIX modelling indicated a strongly negatively buoyant plume comprised almost entirely of fine sediments (Table 4) was vertically discharged from the outlet. The modelled flow was initially dominated by the effluent momentum (jet-like) and was weakly deflected by the ambient current and after some distance the discharge buoyancy became the dominating factor (plume-like). The weakly bent jet plume impinged on the layer boundary (seabed) spreading radially some distance upstream against the ambient flow and then laterally across the ambient flow.

For the 50% percentile (P_{50}) of measured current speeds (see Fig. 6F) the dilution rate at the end of the vertical phase was 1388× indicating possible TSS centreline levels of 180 mg L^{-1} at the boundary level (seabed). The plume then spread laterally in an x and y plane, but more westerly given the currents (used in the model), reaching a distance of 85 m by the end of the near-field plume phase. The plume half-width (y-axis spread) at this point was 21 m, and the dilution rate at the end of the spreading phase was 2359× from the initial starting concentration (250 g L^{-1}), indicating possible TSS centreline levels of 106 mg L^{-1} (Table 6). The model outputs for different current speeds (P_{10} and P_{90}) showed that the plumes always contacted the seabed, with dilution at the end of vertical phase 560 and 1525 times and predicted centreline concentration of 446 and 164 mg L^{-1} respectively (Table 6). Under a faster current speed (P_{90}) the distance of the jet centreline axis from the vertical axis of the discharge line (m) was ~2.8× further than the P_{10} current scenario and the dilution at the end of the vertical phase was also ~2.8× more.

The near-field model was re-run with a hypothetical seabed of 500 m and under a 23 m discharge depth, a P_{50} current speed scenario, the same parameters in Table 6 and the same vertical density distribution. The trapping depth of a single 15 min mud pit discharge was −94 m, or ~15 m lower than the existing seabed (78 m). Re-running the same model scenario but without a 15-minute interval between discharges i.e., as 6 × 15 min = 90 min of continuous discharge, resulted in a −150 m trapping depth.

The far-field model was dynamically coupled to the near-field output at the end of the vertical phase by re-distributing the CORMIX muds pit discharges into the 3 deepest model layers, considering the local current and the horizontal and vertical spatial mass distribution, in the following proportion: 40% (σ = 8, bottom), 30% (σ = 7), 20% (σ = 6) and remaining 10% in layers (σ = 3, 4 and 5).

Modelled TSS levels for a sequence of 6 × 15-minute discharges are shown in Fig. 8A for the NW transect. The transect was chosen given the predominantly NW current flow at the discharge site (Fig. 6G). Modelled TSS levels are for 1 min after the first and second 15-minute discharge events ended, and 60 min after the last (i.e., 6th) discharge ended. Max TSS levels were <25 mg L^{-1} at the model observation point 500 m away from the drill centre, and <15 mg L^{-1} at the 1000 m points (Fig. 8C). Collectively the figures show the generation and movement of detached plumes (caused by the intermittent discharges) indicating the short-term duration and maximum likely TSS levels as the plumes pass over.

The modelled sediment accumulation as a result of all (n = 36) drilling fluid discharges from the 17.5″ sections (where >90% of material was <62.5 μm, Table 4) showed a general northward movement. Deposition levels >~2 km from the drill centre were typically very low <0.1 × 10^{-3} kg m^{-2} (Fig. 8C).

2.7. Ecological surveys

2.7.1. Video surveys (via ROV) around the drill centre

Pre-drilling observations from the ROV video surveys (8 × 200 m transects) radiating out from the drill centre, showed the seabed sediments were generally muddy and covered in a light brown phytodetrital aggregate. Some areas were quite bioturbated with marks and indentations and occasional patches of shallow and sometimes deep circular pit marks (Fig. 9A), caused by feeding and irrigating process associated with the benthic infauna and fish (Rhoads, 1974). The epibenthic taxa were very sparse but typically clumped and comprised of mixed filter feeders such as sea whips, sea fans (gorgonians), other soft corals, sponges and hydroids (Fig. 9B). No photoautotrophs (symbiotic corals, algae or calcareous algae) were present. Sponge growth forms included all of the coarse functional morphologies (see Schonberg and Fromont (2014)); however, the massive, cup-like and erect forms (laminar and palmate) that sit proud of the sediment surface were most prominent. Fan-shaped sponges and gorgonians had the same orientation, with their primary axis aligned in a WSW to NNE direction, perpendicular to the prevailing seabed currents. Colonial hydroids were another conspicuous fauna anchored in the sediments on long flexible stems often surrounded by circular depressions or imprints on the seabed several mms deep (scratch circles see Jensen et al. (2018)) These were presumed to have been caused by contact of the hydroids with the surface creating scour marks from changes in current direction (Fig. 9C).

Post-drilling the seabed and sediment characteristics and filter feeder communities were substantially altered close to the wells. There was a significant quantity of very fine, loose, dark grey unconsolidated sediment with a distinct wave-like rippled pattern (Fig. 9D), which transitioned to a more hexagonal shape further away from the drill centre (Fig. 9D, see also images in S8). This area was largely devoid of all epibenthic fauna. Further along the survey lines the seabed appeared smoother. Scour holes around more consolidated surfaces were filled in with fine sediment, as were the seabed pits and depressions from bioturbation and circular whorls around the hydroids. A veneer of fine grey sediment was observed on top of the previously brown phytodetritus layer along the length of each transect (S8).

Surveys in August 2017 (post-drilling) showed clear loss of soft corals, sponges and hydroids especially close to the drill centre (within the first 50 m, Fig. 10). Further away from the drill centre, cup and

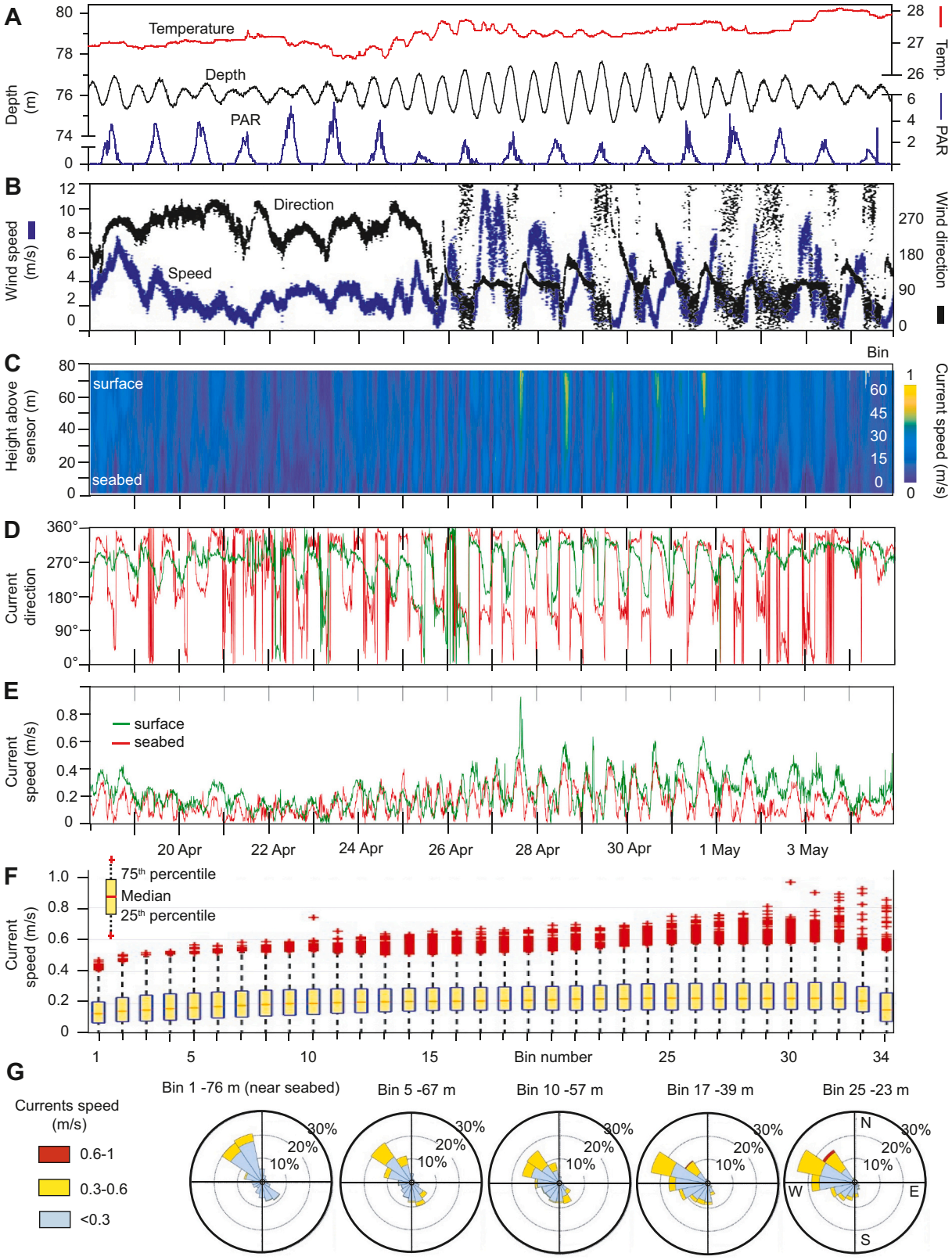

Fig. 6. Hydrometeorological conditions from 18 April to 5 May 2017 during the drilling of the 17.5″ sections (see Fig. 2) showing: (A) depth (m), temperature (°C) and underwater photosynthetically active radiation (μmol quanta m^{-2} s^{-1}), (B) surface windspeed (m s^{-1}), (C) current velocity (m s^{-1}) estimated from the ADCP for the entire water column, as well as (D) direction and velocity direction in the first and last ADCP monitoring bins, (F) box and whisker plots per bin of current speed (where whiskers represent maximum and minimum and red crosses are outliers defined as values more than 1.5× the interquartile range) (G) current roses showing speed (m s^{-1}) and direction distributions for bins 1, 5, 10, 17 and 25 averaged over the deployment period. (For interpretation of the references to colour in this figure legend, the reader is referred to the web version of this article.)

Table 5
Near-field modelling. Cuttings (CUTS) and drilling fluid (MUDS) model input information.

	Units	Near-field model (CORMIX)		Far field model (Delft3D)	
		CUTS	MUDS	CUTS	MUDS
Total mass discharged	t	Na	Na	2540	529
Total mass discharge per individual event	kg	10,800	17,647	See text	
Discharge scenario	S	3600	900		
Mean discharge rate	kg s^{-1}	3.00	19.6	3.00	19.6
PSD/fall velocity		5 classes (cuttings) and 9 classes (muds) Table 4, Fig. 3D			
Outfall diameter and orientation	m	0.3175/90°		See text	
Discharge and water column depth	m	−23, −78.5			
Wind speed/direction	m s^{-1}	2, W		4/SSW	
Local current speed	m s^{-1}	0.11, 0.21, 0.38		See text below	
Local current direction	m s^{-1}	West			
Manning coefficient	$s/m^{1/3}$	0.009		0.01	
Resuspension	N/m^2	Na		0.25	
Water density	kg m^{-3}	Fig. 4D			

barrel shaped sponges containing fine sediments were observed, and also sponges covered by sediment (Fig. 9E, F). Dead sponges and discoloured (grey) gorgonians were noted in the post-drilling images but not in images taken before the drilling program.

Although the ROV transects ran along the same bearing in each survey, the occasional sideways drift of the ROV made it difficult to relocate the same individual fauna or even clusters of individuals through time. However, where this was possible was at the end of transect line 6 (SW bearing from the drill centre) where the sonar marker buoy happened to be located beside a cluster of sponges and gorgonians. The images show the same cluster of individuals before during and after drilling, but with a smooth veneer of sediment on the seabed (Fig. 9G–I).

S8 contains still images before and after the drilling at ~20 m intervals along transect line 8 on a NW bearing from the drill centre (Fig. 8).

2.7.2. Towed video surveys at Rankin and Glomar

In the towed video surveys across Rankin Bank and Glomar Shoal, there was high variability at the scale of individual transects in the composition of biotic categories, as typically several different habitat types were traversed within a 1.5 km transect (see S1 for a schematic representations of habitats). At the shoal level, cover of hard coral, soft coral and other organisms increased slightly both at Rankin and Glomar between the two surveys and sponge cover remained stable at Rankin Bank but decreased slightly at Glomar Shoal (A). Macroalgal cover decreased considerably between the pre- and post-drilling surveys at both Rankin and Glomar (Fig. 11A) and since algae can be highly ephemeral and the change is most likely due to different sampling times (seasonal), the benthic group 'algae' was omitted from further analyses.

At Rankin, towed video transects 1–5 surrounding the drill centre supported similar benthic composition to ROV transects although some hard coral was present on the shallower parts of these transects (S9). Average biotic cover dropped marginally (4.9% to 4.3%) between pre- and post-drilling surveys. Slightly further away from the drill centre and on a semi-protected deeper secondary plateau (55–70 m depth), transect 13 had the highest hard coral cover of any transect at Rankin or Glomar supporting flat disc-shaped solitary corals (predominantly *Diaseris*, Family Fungiidae) and fragile foliose corals (predominantly *Leptoseris* and *Pavona*, Family Agariciidae) (S9). On transect 13, hard coral cover rose between pre- and post-drilling surveys (42.7% to 56.6%) and also on transect 12, which supports a similar high cover mesophotic coral community (34.6% to 47.8%).

Based on benthic community composition, transects from Rankin Bank fell into multiple groups defined by the SIMPROF test largely

Table 6
CORMIX simulation results for the MUDS scenario from a −23 m discharge line under 3 different current speeds of 0.11, 0.21 and 0.38 m s^{-1} (representing the P_{10}, P_{50} and P_{90} of the measured currents).

	m s^{-1}	MUDS		
Current percentile (*P*)		P_{10}	P_{50}	P_{90}
Current speed		0.11	0.21	0.38
Vertical phase (jet module)				
Vertical extent of the jet region	m	Seabed	Seabed	Seabed
Distance of the jet centreline axis from the vertical axis of the discharge line	m	21	65	97
Dilution rate at end of the phase	×	560	1388	1525
Possible centreline TSS	mg L^{-1}	446	180	164
Spreading phase (spreading module)				
Lateral distance at the end of the spreading phase	m	219	85	113
The plume half-width (i.e., y-axis spread)	m	396	21	16
Dilution rate at end of the spreading phase	×	1431	2359	2592
Possible centreline TSS at the end of spreading phase	mg L^{-1}	175	106	96

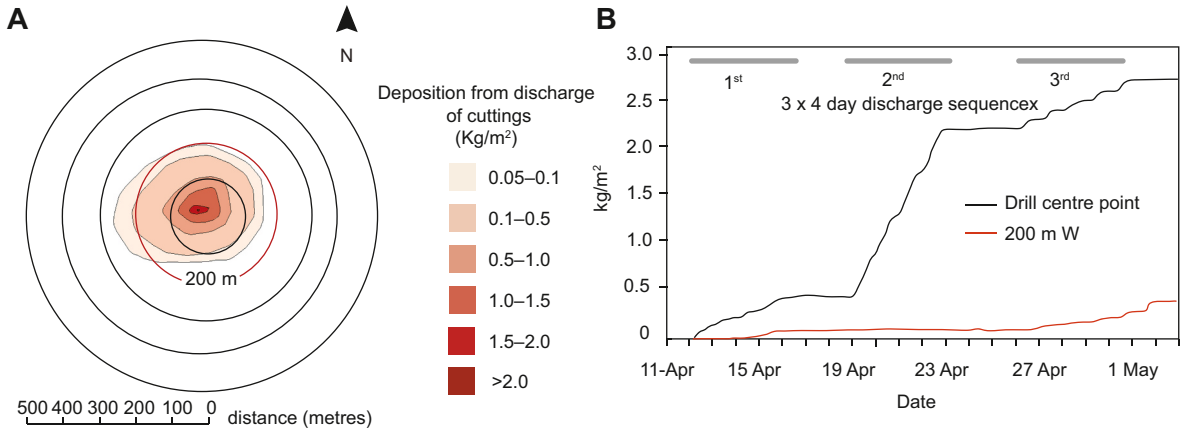

Fig. 7. (A) modelled cuttings accumulation on the seabed (kg m^{-2}) for the 3 × 17.5″ sections (where 80% of the bottom-hole section cuttings were discharged) 2 days after of the last cuttings discharge (B) time series of sediment accumulation at the drill centre and at 200 m West of the drill centre over the batch drilling of the 17.5″ sections. (For interpretation of the figure legend, the reader is referred to the web version which is in color).

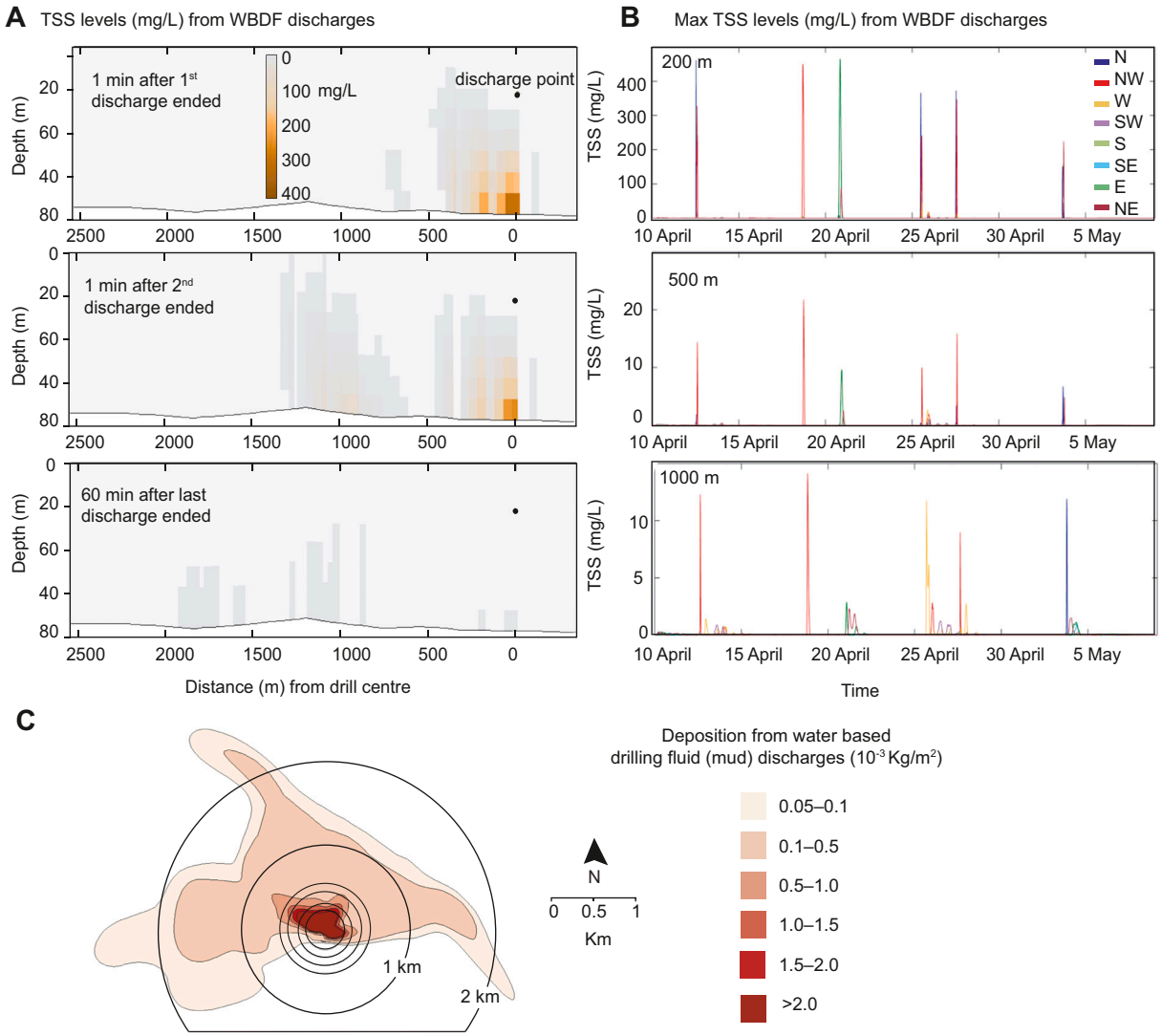

Fig. 8. (A) Simulated TSS levels (mg L^{-1}) from a sequence of 6 mud pit discharges (each lasting 15 min) on 12 April (see Fig. 2) from 1 min after the first discharge started to 60 min after the sixth discharge ended, (D) simulated maximum water column TSS levels (mg L^{-1}) from 10 April to 5 May at points 200, 500 and 1000 m away from the drill centre in a N, NW and W direction. (C) Modelled seabed sediment accumulation from all mud pit discharges from the 17.5″ sections (i.e. 36 discharge events) in 10^{-3} kg m^{-2}, centred on the drill centre for discharges released 30 min after low water (see text) on each day. (For interpretation of the figure legend, the reader is referred to the web version which is in color).

associated with depth strata and reflecting differences in hard coral cover (Fig. 11B). Most transects remained within the same SIMPROF groups for pre- and post-drilling surveys and of note, the coral diversity in deep water at the five transects nearest the drill centre (transects 1–5) remained similar between the pre- and post-drilling surveys (although there was a drop in cover of hard coral on transect 3 from 4.4% to 1.4%), and variations in percentage cover at Rankin Bank were similar to those seen at the control location, Glomar Shoal (Fig. 11B, S9). The PERMANOVA confirmed there were significant differences between transect, location, the interaction of depth × transect and depth (S9), but notably survey time (pre-drilling v post-drilling) was not significant either as a single factor or in combination with location or transect (S9).

2.7.3. *Baited remote underwater video stations (BRUVS)*

A total of 15,616 individual fish were recorded across Rankin and Glomar (representing 53 families and 330 species). A greater number of individuals and species (291 species) were recorded at Rankin compared to Glomar (196 species, Fig. 12A). Despite twice the number of BRUVS deployed at Rankin, mean species richness and abundance were considered similar at both locations (Fig. 12A). Within each shoal, richness and relative abundance was highly variable between pre- and post-drilling BRUVS deployments at each BRUVS site. Yet overall, species richness (Fig. 12B) and relative abundance (Fig. 12C) were similar between pre- and post-drilling surveys at both shoals, and no clear trend could be associated with the drilling campaign (Fig. 12).

Likewise, for the subset of 13 BRUVS sites at Rankin closest to the drill centre (distance 2–3 km, video transects 1–5), no clear trends in fish indices were observed pre- and post-drilling: richness and relative abundance were higher after the drilling campaign at 7 sites, lower for 5 sites, and remained stable for one site. Mean richness was similar overall between surveys (16 ± 2 species pre-drilling, 18 ± 2 species post-drilling) at these sites in closest proximity to the drilling activity and were lower than shoal-scale averages (Fig. 12B) since these sites were deep (65–90 m) and comprised low complexity habitat. High variability was observed in relative abundance between surveys (10–282 individuals per BRUVS) at the BRUVS sites closest to the drill centre. Over 200 individuals, primarily the schooling trevally *Gnathanodon speciosus* and *Rhabdamia* cardinalfishes, were recorded at two sites during the post-drilling survey, likely associated with opportunistic sampling or BRUVS being positioned in different microhabitats. Thus, mean relative

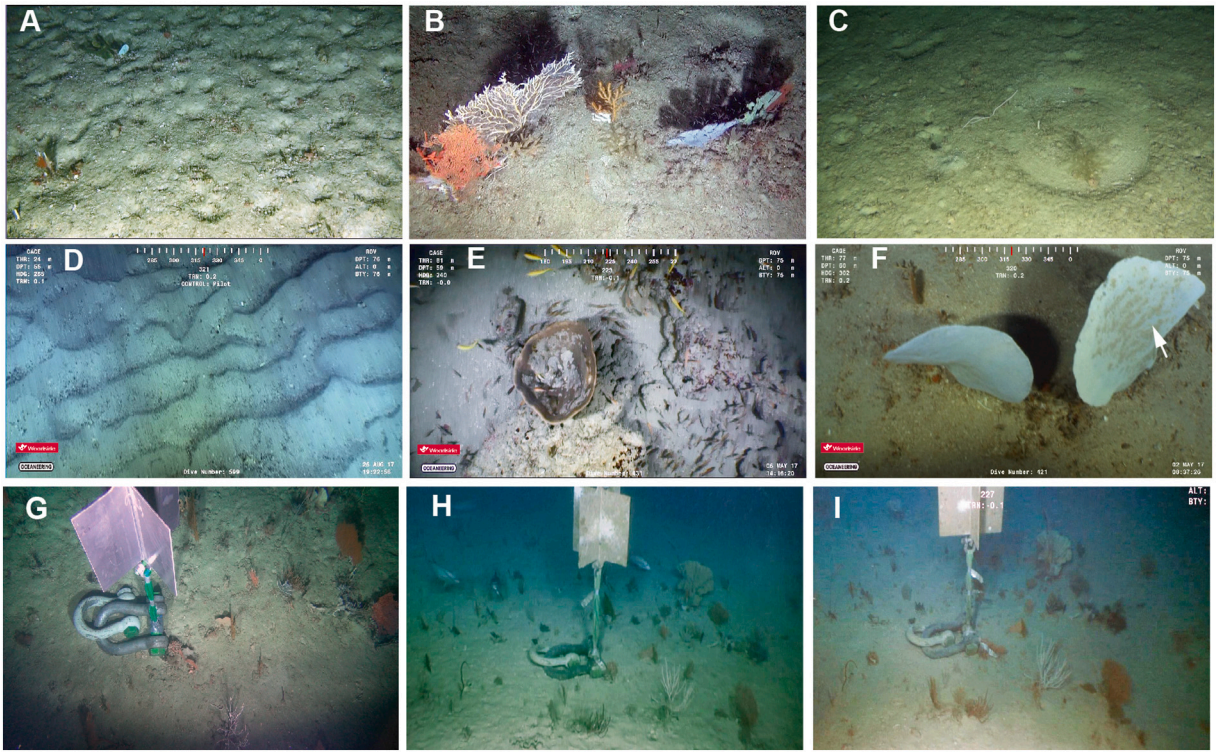

Fig. 9. Still images from the downward facing HDTV on the ROV showing epibenthic communities within 200 m of the drill centre. Before drilling (November 2016) showing: (A) depressions (hollows) in the seabed from bioturbation, (B) clusters mixed epibenthic taxa primarily soft corals, gorgonians (sea fans) and sponges, (C) distinctive circular, imprints (scratch circles) on the seabed caused by stalked hydroids. After drilling (April to May 2017) showing: (D) seabed ripples and loose fine sediment 50 m away from the drill centre, (E) sediment accumulation in barrel sponges, (F) sediment attached to sponges (see arrows). (G, H, I) forward-facing imagery at the end of transect line 6 (SW direction) 200 m away from the drill centre, before (November 2016), during (May 2017) and after (August 2017) drilling.

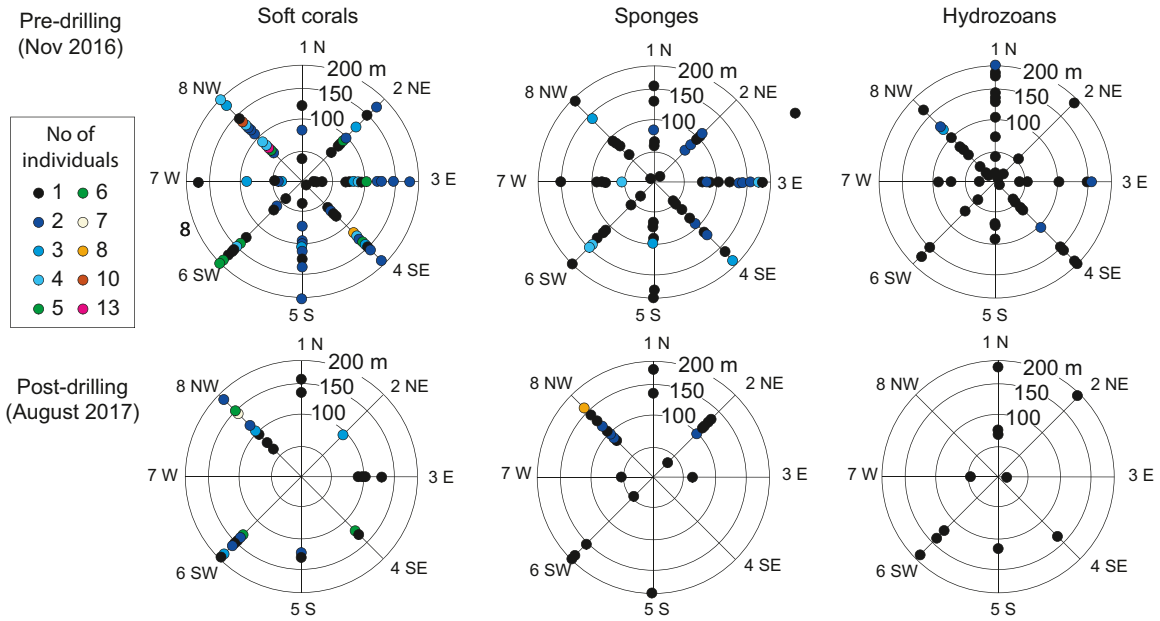

Fig. 10. ROV seabed surveys around the drill centre showing polar plots of soft corals, sponges and hydrozoans along the environmental survey lines before (November 2016), and after (August 2017) the drilling program. Each dot represents the number of points (out of 20 per image) overlying a soft coral or sponge in the point-intercept method, or individual hydroids hydrozoans from the 30 still images captured from the ROV HDTV video footage of the benthos along each 200 m transect (see Fig. 1D).

abundance was greater during the post-drilling survey (78 ± 26 individuals), although was similar overall between surveys with exclusion of these two records (>200 individuals: 44 ± 9 individuals pre-drilling, 41 ± 9 post-drilling).

Depth category and local relief (rng50) were significant predictors ($p < 0.05$) explaining fish community structure at Rankin at the shoal-

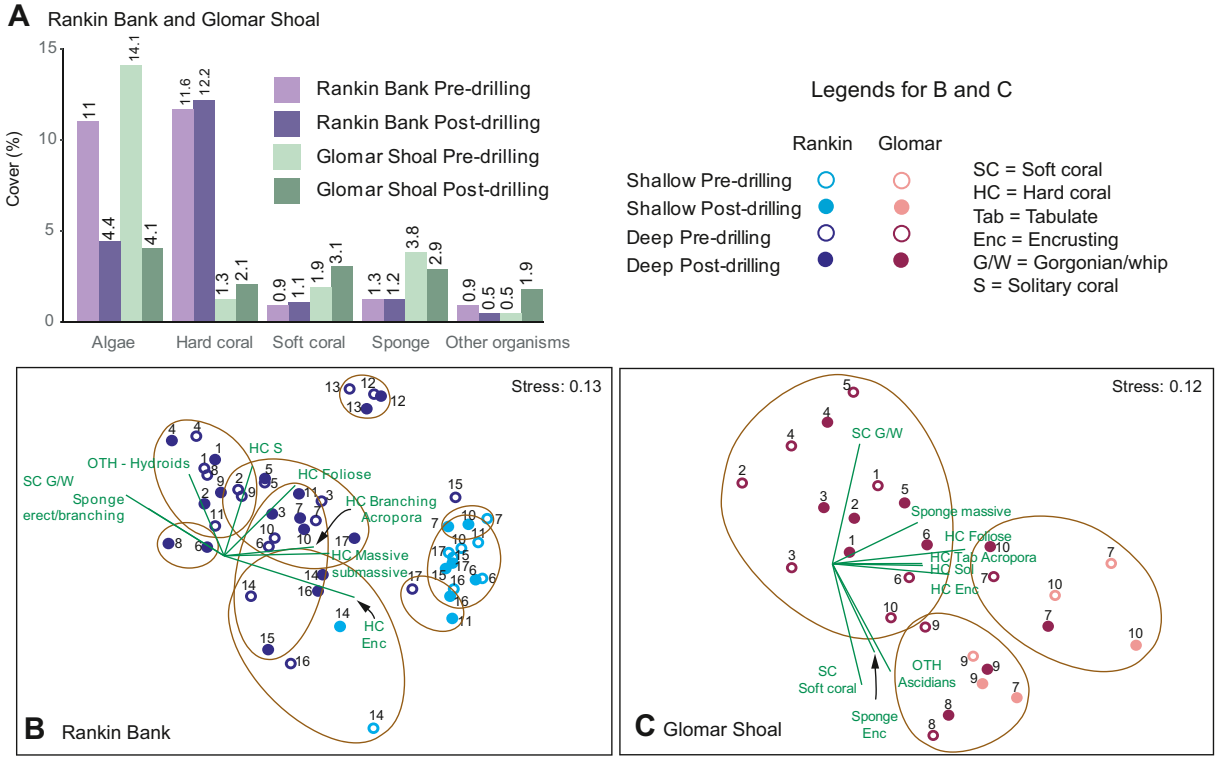

Fig. 11. (A). Abundance (total % cover) of the five major categories of biota for Rankin and Glomar, comparing pre- and post-drilling. (B, C) Two-dimensional representation of a multidimensional scaling (nMDS) ordination of transects based on the cover of fine-scale categories at Rankin Bank and Glomar Shoal. Data were square root transformed and a Bray-Curtis similarity matrix constructed prior to analysis. The plot is overlaid with SIMPROF groups from the cluster analysis and vectors for fine-scale benthic categories with correlation >0.2.

scale, with the dbRDA model based on composition of fish genera explaining 42% of the variation (Fig. 12D, S10). The model for Glomar (57% variation explained) indicated depth category, encrusting cover and local relief were significant in explaining the fishes observed (Fig. 12E, S10). There was no separation of points based on pre- or post-drilling surveys and the marginal effect of survey and Ba concentrations (derived from nearby sediment sampling sites and indicating drilling mud exposure) were non-significant in dbRDAs, thus no effect of survey or Ba concentrations on the composition of fishes was evident (Fig. 12, S10). Greater species richness was observed at shallow sites, and fish genera common to shallow depths associated with structural habitat, e.g., *Sufflamen* triggerfishes, and *Lethrinus* emperors and *Bodianus* hogfishes. In contrast, *Abalistes* triggerfishes and *Pristipomoides* snappers characterised the deeper bare habitat at both shoals (Fig. 12A and B). Examination of the 13 BRUVS sites closest to the drill centre, survey and Barium were also not significant in the dbRDA model, cover of filter-feeder benthos was the sole significant predictor in explaining the composition of fish genera (66% of the variation explained, S10).

3. Discussion

The study was undertaken to improve knowledge and provide guidance on reducing uncertainty with plume dispersion model and impact predictions when drilling near sensitive environments. Of the different discharges the behaviour of the high volume, high emission rate (sensu Ayers et al., 1982) mud pit discharges was focused on as these discharges have the greater potential for longer-range transport hence for environmental contamination (sensu Chapman, 2007). Near- and far-field models were coupled to describe the discharge trajectories and areal extent of effects using actual volumes, concentrations, discharge durations and site-specific sediment fall velocities as well as time and site-specific hydro-meteorological conditions (as recommended by Nedwed (2004); Niu et al. (2009); Pivel et al. (2009); Rye et al. (2008)). Proxy estimates of TSS were made using ROV-based turbidity measurements in the discharge plumes to validate nearfield model predictions (Frost et al., 2014; Rye and Furuholt, 2010). Overall, the effects were found to be local, partly because of the comparatively shallow depths but also because of the distinct behaviour of the drilling mud discharges on release. The study emphasized the need to better characterise the discharges of drilling muds including the timing and duration and sequence of discharges, as well as volumes and concentrations for future drilling near sensitive environments (see Frost et al. (2014); Rye and Furuholt (2010)).

In this drilling campaign the bulk of the discharges were associated with the 17.5″ sections and the discharge of cuttings and drilling fluids was from the MODU at the surface where there is a greater possibility for wider dispersal than discharging at the seabed. For the drilling fluids, losses from solids control equipment, and fluids adhered to drill cuttings represented important pathways, but the majority (95%) of the drilling fluid losses occurred from the high volume, high discharge rate, planned mud pit discharges (mud pit dumps). Since there was a need for two fluid systems (gel-polymer and KCl-polymer) for each of the 17.5″ sections, and a requirement to switch between the two systems for each well, there were several periods of multiple bulk WBDF discharges -. When these factors were coupled to the close (spatial and temporal) proximity of the three-well batch drilling campaign, the greatest potential risk of the movement of discharges into the shallower more biodiverse, mesophotic reefal environment was considered to be the 17.5″ sections – which were targeted in the study. The potential ecological effects on epibenthic fauna from coarse cuttings and fine drilling fluid discharges (bentonite, barite, formation solids) is primarily explained in terms of smothering and physical burial (Durgut et al., 2015; Purser, 2015; Schaanning et al., 2008; Smit et al., 2008; Vad et al., 2018) although elevated TSS levels are also a well-known hazard for filter feeder communities (Bell et al., 2015; Pineda et al., 2017b). Biological and sedimentary effects are discussed in conjunction below, first in terms of

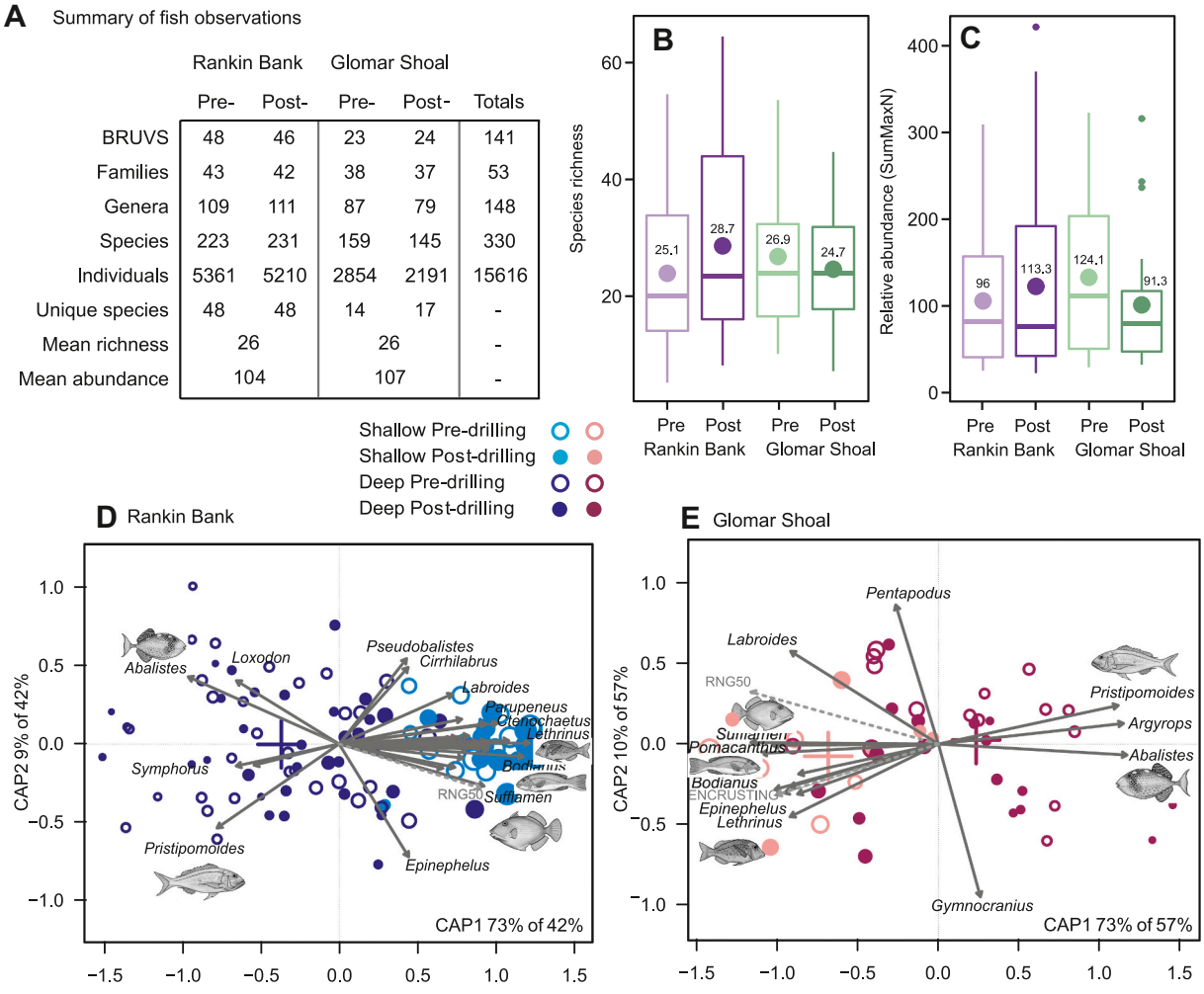

Fig. 12. BRUVS observation summary (A) indicates number of deployments, and fish indices by survey. Boxplots indicate interquartile ranges and outliers in fish species richness (B) and raw relative abundance (C) by survey and shoal. Centre lines indicate medians, means are symbols and values within the boxes. Redundancy analysis (dbRDA) biplots from show fish genera occurring on at least 5% of samples at (A) Rankin (87 genera) and (B) Glomar (92 genera). Survey (pre-drilling: open circles; post-drilling closed circles), depth category (points and centroids coloured as shallow: light blue/pink; deep: dark blue/dark red) and significant predictors (dashed lines) are displayed. Weighted averages of site scores (point size) are scaled by site richness. Significant genera vectors ($p < 0.001$, solid lines) correlated with linear constraints are listed in S10, and fish images highlight five of the genera common to both shoals. (For interpretation of the references to colour in this figure legend, the reader is referred to the web version of this article.)

cuttings discharges and then drilling fluids and then links to the biological responses.

Cuttings are functionally analogous to the used drilling fluids i.e., as seawater slurries of solid particles containing different quantities of the various additives from drilling fluid adherence. However, they differ considerably in particle size (as a result of the solids control equipment) and in behaviour once released. Over 95% of the cuttings were greater than 1 mm (and >35% >2 mm) and the settling time to the seabed was minutes to tens of minutes. The CORMIX modelling predicted a mostly circular deposition zone and because of the fast settling velocities, comparatively shallow seabed depth (78 m) and relatively deep discharge point (−23 m), the deposition field was largely constrained to a few hundred metres under the majority of the measured current speeds. The cuttings deposition field aligned with observations from the ROV out to the 200 m safe limits of the ROV tether (see further below). Rye and Furuholt (2010) describe a similar size footprint for a drilling program in Norway where empirical and modelled data were collected and compared to track discharge dispersion and fate. Similar localized deposition fields from cuttings discharges have been described previously (Bakke et al., 2013; IOGP, 2016 and references therein), consistent with the results of this study.

For the drilling fluids, the behaviour of the discharges was very different, with ROV footage showing the generation of well–defined negatively buoyant dynamic near-field jets with a high initial momentum on release from the mud pits. The distinctive cloud-like plume descended rapidly, entraining water and growing in diameter (billowing) with increasing depth, eventually reaching the seabed. Drilling fluid discharge rates from these mud pit dumps were very high at 20 kg s^{-1}, or >6.5× greater than the cuttings discharge rates from the 17.5″ sections and 25× higher than cuttings discharges from the subsequent lower sections of the wells. Supporting the in situ observations, the CORMIX model described a jet-plume and the vertical phase of the plumes always impinged on the layer boundary (i.e., the seabed) under all current velocities tested.

Confirming the near-field model predictions is very challenging as in situ water sampling for gravimetric analysis of TSS can only ever provide a few samples of a highly dynamic situation. For this reason, proxy estimates of TSS levels were made using continuous turbidity measurements from a nephelometer mounted to the ROV which repeatedly profiled the descending plumes. Nephelometers are sensitive to different sediment types and particle size distributions (Davies-Colley and Smith, 2001), but in this study the relationship between NTU and TSS proved to

be linear over the range of hundreds of mg L^{-1} and was also consistent despite sampling different water-based drilling fluid types. This was probably because the solids control equipment on the MODU maintained the mud with a uniform PSD. It could also be that once the different mud types had been used during drilling the solid content (from the formations) was higher and they converged on a similar state as shown by the microscopy. The net effect was a very uniform PSD of fine solids in the water column, which was very favourable for use of nephelometry as a proxy or surrogate measure of TSS (Frost et al., 2014).

Estimated TSS levels within the plumes were very variable and there is no guarantee that the jet centreline concentration predicted by the near-field model was sampled during the ROV profiling. Therefore, it is only possible to say that the centreline value must be equal or greater than the maximum proxy TSS level estimated at that depth and time. From an initial (pre-release) mud pit concentration of 250,000 mg L^{-1}, and from convective descent and entrainment of ambient water, the minimum centreline value of the plumes at depths of up to 35 m was estimated to be >600 mg L^{-1} (the maximum resolution of the nephelometer), 200–500 mg L^{-1} at 40–50 m depth and 100–200 mg L^{-1} near the seabed (at 60–78 m). These measured values closely align to the CORMIX model predicted centreline concentrations of up 180 mg L^{-1} above the seabed under the median current flow. Thus, both modelled and empirical measurements suggest a >3 order of magnitude dilution from the initial discharge before contact with seabed biota tens of metres away from the vertical axis of the discharge line depending on current speed.

The convective descent of the mud pit discharges simulated by the CORMIX nearfield model was coupled to a far-field model to capture the movement of the passive plume. The coupled models recreated the series or train of smaller connected plumes stemming from the sequence of intermittent mud pit discharges. An initial NW flow was predicted, reflecting the predominance of strong WNW to NW current flow over the drilling of the 17.5″ sections. Modelled TSS concentrations up to 10 mg L^{-1} were possible 1000 m away from the discharge point but over a period of minutes as the successive discharges intermittently passed through the area over a few hours (see also Purser (2015)). For contextual purposes maximum hourly TSS levels 200–500 m from capital dredging projects can exceed hundreds of mg L^{-1} and occasionally average >100 mg L^{-1} over a 24-hour period (Fisher et al., 2015). Transient peaks in TSS levels of tens or hundreds of mg L^{-1} for a few hours are common during cyclones and storms in tropical shallow water reef environments (Abdul Wahab et al., 2017; Fisher et al., 2015). In a study of the inshore reef environments of the Great Barrier Reef, TSS levels exceeded 150 mg L^{-1} from natural wind/wave resuspension and averaged 17 mg L^{-1} for a 2-week period (Whinney et al., 2017).

The ROV based observations supported the model studies and a notable feature of the seabed was the wave-like rippling near the drill centre caused from a build-up of cuttings and muds (Jones et al., 2012). This area was up to ~50 m from the drill centre and was effectively devoid of all epibenthos. The initial seabed patterning is indicative of post settlement re-suspension and transport processes that was not addressed in the modelling (or in most discharge modelling). Outside the area and with increasing distance from the wells, the rippling transitioned to a tile-ripple shape (cf Roos and Blondeaux (2001)) and then lost definition, changing to a gradually thinning veneer of fine sediments covering the seabed phytodetrital layer, bioturbation marks and generally smoothing the seabed surface.

The modelled and observed behaviour of the drilling fluid plumes were also supported by chemical analyses of the seabed. Barite is used as a weighting agent in drilling fluids to increase the mud density, and comprises a significant component of some muds (National Research Council (US), 1983). Environmental contamination with barite from drilling fluids is well recognized and barium has been frequently used as a tracer of drilling fluid discharges (Ellis et al., 2012; Kennicutt et al., 1982; Phillips et al., 1998; Purser, 2015) and for model validation (Rye et al., 2006). Barite was only used in the 17.5″ and 12.25″ sections and since the NADF from the 12.25″ sections was shipped to shore for processing, contamination of the seabed was primarily from the 17.5″ sections. The barium level was highly elevated (3 g kg^{-1}) at the 50 m sampling point along the western transect, representing an enrichment of >260× compared to the reference sites and similar to estimates in seabed sediments surrounding rigs (Frost et al., 2014; Hughes et al., 2010; Junttila et al., 2018; Neff, 2008; Purser, 2015). Barium levels decreased with increasing distance away from the wells to 1.2 and 0.75 g kg^{-1} at the 100 m and 200 m sampling locations (see further below).

Some chromium enrichment around the wells was noted which could be due to drilling fluid additives, trace mineral impurities of the barite and also bentonite clay, or contamination from the sedimentary rocks (drill cuttings) penetrated by the drilling (Crecelius et al., 2007; Edge et al., 2016; Neff, 2010; Neff, 2008). Chromium levels were nevertheless well below Australian (ANZECC/ARMCANZ) SQGs (see Simpson et al. (2013)) which are largely based on the effects range-low (ERL) and effects range-median (ERM) values of Long et al. (1995). There are no SQGs for barium but it has a low solubility in seawater (Burton et al., 1968), and most of the associated metal impurities are in the form of mineralized metal sulphides (Kramer et al., 1980; Leuterman et al., 1997). These have limited environmental mobility and low toxicity to plants and animals (Neff, 2002a, 2002b, 2008). The ultimate fate is probably resuspension (erosion) and transport away from the drilling sites and dilution and diminution over much greater distances.

The drilling occurred on a 78 m deep seabed on the SE flank of Rankin and the maximum noon instantaneous light was <0.4% of a maximum theoretical incident downwelling irradiance based on measurement on a typical clear sky at tropical noon at Cape Lambert on the Pilbara coast at 0.1 m depth (see Jones et al. (2016)). Underwater light levels were thus just below 1% of surface light typically used as a threshold to define the photic zone (Kahng et al., 2019; Kahng et al., 2014; Kirk, 1994; Lesser et al., 2009). No photoautotrophs (including hard corals) were seen in the surveys immediately around the wells, consistent with a previous study showing a transition from phototrophic to heterotrophic communities with depth at Rankin Bank (Abdul Wahab et al., 2018). The naturally muddy seabed around the wells had a very sparse, clumped distribution of mixed epibenthic fauna dominated by sponge and soft coral filter feeders. Although the length of the ROV based HDTV seabed surveys around the drill centre was operationally constrained by the safe tether length, clear biotic environmental gradients were also observed over the 200 m length of the transects.

Overall, the surveys suggest a zone of high impact surrounding the drill centre up to 50–75 m in all directions which would have been caused by cuttings and fluid discharges from the MODU; although, the initial discharges from the riserless top-hole sections that discharged straight to the seabed would also have contributed to some of the zone of high impact. Outside this zone was an area of medium impact up to the ends of the 200 m transect lines where there were clear losses of epifauna, but nevertheless sponges and soft corals were still observed. In this area sponges and soft corals were sometimes observed with sediment attached. Sponges normally keep their surfaces free of sediment and have a number of cleaning mechanisms to remove sediments from their surfaces including mucus production, tissue sloughing, self-cleaning surfaces (Pineda et al., 2017a). Overall, the size of the area of biological change is consistent with previous analyses (Ellis et al., 2012; Jones et al., 2012; Vad et al., 2018).

Of particular interest for drilling close to a sensitive environment is the longer distance movement of the bulk discharged water-based drilling fluids away from the immediate deposition zone associated with the cuttings (from the top and bottom hole sections). Unfortunately, the operational exclusion zone around the MODU (associated with the anchoring system) prevented sampling in an area 200–2000 m around the wells. Nevertheless, barium levels outside the 2000 m exclusion zone were only slightly elevated by a few tens of mg kg^{-1} above the reference site levels, suggesting a longer distance (i.e., kilometres) movement of drilling fluid and as suggested by the drilling fluid discharge modelling.

In a review of many production and exploration wells Ellis et al. (2012) describe the elevated sediment barium concentrations in sediment samples up to 1000 m and 3000 m from the platforms before decreasing to background levels. Barite and bentonite have been referred to as practically inert from a toxicological perspective (Neff, 1987; Smit et al., 2008), and remain on the most recent (July 2019) Oslo and Paris (OSPAR) commission list of substances used and discharged offshore which are considered to pose little or no risk to the environment (OSPAR Agreement 2013-06).

Epibenthic fauna under the influence of the far-field drilling mud plume are estimated to have experienced episodic, intermittent elevations of suspended of >25 mg L^{-1} and only briefly (minutes) as the drilling fluid plumes passed overhead (see also Frost et al. (2014)). Larsson et al. (2013) demonstrated a possible interference on prey capture in a cold water coral *Lophelia pertusa* exposed to a drill cuttings load of 25 mg L^{-1} for 12 weeks of continuous exposure. Using the same species, Baussant et al. (2018) used pulsed exposures every few hours peaking at <50 mg L^{-1} and averaging 25 mg L^{-1} and over a 12 week period. No effects were seen on prey capture and growth in both studies was no different from controls. Although both studies used environmentally realistic concentrations (cf Frost et al. (2014)) the exposure durations were much longer than would be experienced in situ for a single well. Both studies concluded the coral was robust and resilient to drill cuttings showing no major effects over long periods (weeks) at tens of mg L^{-1}. A recent study with five tropical sponge species exposure to elevated sediment concentrations of ≥23 mg L^{-1} for extended periods (days to weeks) had a negative effect on sponge feeding behaviour with associated depletion of energy reserves. However, ≤10 mg L^{-1} for 28 days was tolerable by most species and was suggested as a sub-lethal threshold in adult sponges (Pineda et al., 2017b).

Modelled total sediment accumulation (mud and cuttings deposition) at 200 m from the drill centre was only up to 0.5 kg m^{-2} (50 mg cm^{-2}) or ~0.5 mm based on a wet bulk density of 1050 kg m^{-3} for recently settled mud (Van Rijn (2007), see also Rye and Furuholt (2010) and Frost et al. (2014)). Given the very low suspended and low sediment accumulation levels when the drilling of the 17.5″ sections was conducted and given the distance between the shallower areas of Rankin and the drill centre was >~5 km, it was not surprising that the pre- and post-drilling epibenthic towed video surveys and BRUVS demersal fish surveys did not detect any changes that could be attributed to the effects of the drilling. There were significant differences between transect, location, the interaction of depth × transect and depth consistent with earlier studies of Rankin and Glomar (Abdul Wahab et al., 2018); however, survey time (pre-drilling v post-drilling) was not significant either as a single factor or in combination with location or transect. Although changes in the relative proportion of benthic categories such as macroalgae at Rankin were seen, these were similar to changes at Glomar, and thus are likely to reflect seasonal variation rather than any effects of the drilling campaign. Similarly, both Rankin and Glomar displayed similar variability in fish species richness and relative abundance, and no clear pattern was identified between pre- and post-drilling surveys at Rankin overall, nor at sites closest to the drill centre. Differences in fish communities at Rankin and Glomar were strongly associated with depth, seabed complexity and habitat, reflecting the relationship between fishes and the patchiness of habitats across the shoal systems. In general fishes are likely less sensitive to drilling discharges than benthic communities attributable to their mobility (IOGP, 2016), and our results did not indicate patterns in fish richness and relative abundance linked to the drilling campaign.

Collectively the analyses provided a coherent story of the effects of the discharges on the surrounding environment, the size and scale of the area influenced, and how to increase confidence in model predictions. As with plume trajectory modelling for coastal dredging operations, there are often many unknowns at the pre-approval environmental impact assessment stage. Informed approximations and generalizations are typically made based on previous experience and the most probable scenarios created (Sun and Branson, 2019). With the benefit of hindsight, in this batch drilling case, the a priori estimates of the cuttings discharges (data not shown) were found to closely approximate what actually occurred during the drilling campaign both in terms of volume and duration of discharges. However, the a priori drilling fluids discharge scenarios (data not shown) were much less fitting in terms of volumes and especially the manner and duration of discharges. The pulsed episodic nature of the discharges from the mud pits was not recreated, and discharge durations were much longer for a smaller volume of muds released. Such scenarios would not have been as conducive to jet formation and convective descent which, as shown in this study, conveyed the muds downwards orders of magnitude faster (i.e., in minutes) than would have occurred by gravity alone (i.e., in days) reducing the opportunity for long range transport. Although used drilling fluids (muds) and cuttings (with drilling fluid adherence) are compositionally similar they behaved very differently when discharged. To increase surety of model outputs it is recommended that the batch and intermittent disposal of drilling fluid discharges are better described and justified in model inputs (Rye et al., 2012) and any nearfield plume formation is better described in interpreting model outputs.

For future drilling near high ecological value, sensitive and iconic environments such as shallow submerged and mesophotic reefs, avoiding any contact of drilling wastes with benthic communities (i.e., contamination) may be just as important as avoiding any biological effects (i.e., pollution). In this study the longer distance movement of drilling waste was associated with the mud pit discharges as opposed to fluid adherence as mud attached to cuttings which was found to be minor (cf Rye et al. (2012)). This offers some opportunities for impact minimisation and reducing risks to as low as reasonably practicable, and acceptable, which is part of the Australian objective-based regulatory regime (IOGP, 2021). Storing used muds and then discharging when tidal currents are moving away from an area of concern could be an option. Similarly using deeper discharge outlets and storing used muds and discharging them continuously, as opposed to intermittently (batches), would encourage deeper trapping depths by greater inertia as shown in this study. Skip and ship operations for WBDFs (see IOGP, 2021) are also an option for disposal away from coral reefs and coral reef mesophotic zones.

Funding

Funding was provided by Woodside Energy Ltd, as operator of the North West Shelf Project Joint Venture, involving BHP Billiton Petroleum (North West Shelf) Pty Ltd, BP Developments Australia Pty Ltd, Chevron Australia Pty Ltd, Japan Australia LNG (MIMI) Pty Ltd, Shell Australia Pty Ltd, and with co-investment from the Australian Institute of Marine Science (AIMS).

CRediT authorship contribution statement

R Jones: funding acquisition, conceptualization, project administration, investigation, formal analysis, visualization, writing – original draft, writing – review & editing, M Wakeford: formal analysis, visualization data curation and writing, L Currey-Randall: formal analysis, visualization data curation and writing, Karen Miller: funding acquisition, field work. Hemerson Tonin: methodology, formal analysis and visualization, writing. All authors approved the final submission.

Declaration of competing interest

The authors declare that they have no known competing financial interests or personal relationships that could have appeared to influence the work reported in this paper.

Acknowledgement

Woodside is acknowledged for providing access to the daily mud reports, operational discharge logs, daily drilling reports and end of well environmental discharge reports. Technical and logistical support is acknowledged from Max Rees, the ROV operators Oceaneering (Perth), the MODU operators Diamond Offshore, and the Drilling & Completions teams of Woodside GWF-2 project. Denise McCorry (WEL) is acknowledged for instigating and enabling this investigation.

Appendix A. Supplementary data

Supplementary data to this article can be found online at https://doi.org/10.1016/j.marpolbul.2021.112717.

References

Abdul Wahab, M., Fromont, J., Gomez, O., Fisher, R., Jones, R., 2017. Comparisons of benthic filter feeder communities before and after a large-scale capital dredging program. Mar. Pollut. Bull. 122, 176–193. https://doi.org/10.1016/j.marpolbul.2017.06.041.

Abdul Wahab, M.A., Radford, B., Cappo, M., Colquhoun, J., Stowar, M., Depczynski, M., Miller, K., Heyward, A., 2018. Biodiversity and spatial patterns of benthic habitat and associated demersal fish communities at two tropical submerged reef ecosystems. Coral Reefs 37, 327–343. https://doi.org/10.1007/s00338-017-1655-9.

Anderson, M., Gorley, R.N., Clarke, R.K., 2008. Permanova for Primer: Guide to Software and Statisticl Methods. Primer-E Limited, Plymouth, UK.

Ayers, R.C., Meek, R.P., Sauer Jr., T.C., Stuebner, D.O., 1982. An environmental study to assess the effect of drilling fluids on water quality parameters during high-rate, high-volume discharges to the ocean. J. Pet. Technol. 34, 165–173.

Bakke, T., Klungsøyr, J., Sanni, S., 2013. Environmental impacts of produced water and drilling waste discharges from the norwegian offshore petroleum industry. Mar. Environ. Res. 92, 154–169. https://doi.org/10.1016/j.marenvres.2013.09.012.

Baussant, T., Nilsen, M., Ravagnan, E., Westerlund, S., Ramanand, S., 2018. Effects of suspended drill cuttings on the coral Lophelia Pertusa using pulsed and continuous exposure scenarios. J. Toxic. Environ. Health A 81, 361–382. https://doi.org/10.1080/15287394.2018.1444375.

Bell, J., McGrath, E., Biggerstaff, A., Bates, T., Bennett, H., Marlow, J., Shaffer, M., 2015. Sediment impacts on marine sponges. Mar. Pollut. Bull. 94, 5–13. https://doi.org/10.1016/j.marpolbul.2015.03.030.

Birt, M.J., Stowar, M., Currey-Randall, L.M., McLean, D.L., Miller, K.J., 2019. Comparing the effects of different coloured artificial illumination on diurnal fish assemblages in the lower mesophotic zone. Mar. Biol. 166, 154. https://doi.org/10.1007/s00227-019-3595-0.

Burton, J., Marshall, N., Phillips, A., 1968. Solubility of barium sulphate in sea water. Nature 217, 834.

Cappo, M., Harvey, E.S., Shortis, M.R., 2007. Counting and measuring fish with baited video techniques-an overview. In: Australian Society for Fish Biology 2006 Workshop Proceedings. Australian Society for Fish Biology, pp. 101–114.

Cappo, M., Speare, P., De'ath, G., 2004. Comparison of baited remote underwater video stations (BRUVS) and prawn (shrimp) trawls for assessments of fish biodiversity in inter-reefal areas of the great barrier reef Marine Park. J. Exp. Mar. Biol. Ecol. 302, 123–152. https://doi.org/10.1016/j.jembe.2003.10.006.

Chapman, P.M., 2007. Determining when contamination is pollution — weight of evidence determinations for sediments and effluents. Environ. Int. 33, 492–501. https://doi.org/10.1016/j.envint.2006.09.001.

Clarke, K., Gorley, R., 2015. Primer Version 7: User Manual/Tutorial. PRIMER-E, Plymouth, UK.

Clarke, K.R., Somerfield, P.J., Gorley, R.N., 2008. Testing of null hypotheses in exploratory community analyses: similarity profiles and biota-environment linkage. J. Exp. Mar. Biol. Ecol. 366, 56–69. https://doi.org/10.1016/j.jembe.2008.07.009.

Commonwealth of Australia, 2010. Australian Energy Resource Assessment. Department of Resources Energy and Tourism (DRET), Australian Bureau of Agricultural and Resource Economics (ABARE), and Geoscience Australia (GA). ISBN 978-1-921672-59-0, Canberra, Australia, 358 pp. pp. https://d28rz98at9flks.cloudfront.net/70142/70142_complete.pdf.

Commonwealth of Australia, 2012. pp. In: Marine Bioregional Plan for the North Marine Region - Prepared Under the Environment Protection and Biodiversity Conservation Act 1999. Department of Sustainability, Environment, Water, Population and communities (SEWPAC), p. 269. http://www.environment.gov.au/system/files/pages/1670366b-988b-4201-94a1-1f29175a4d65/files/north-west-marine-plan.pdf.

Cordes, E.E., Jones, D.O., Schlacher, T.A., Amon, D.J., Bernardino, A.F., Brooke, S., Carney, R., DeLeo, D.M., Dunlop, K.M., Escobar-Briones, E.G., 2016. Environmental impacts of the deep-water oil and gas industry: a review to guide management strategies. Front. Environ. Sci. 4, 58.

Crecelius, E., Trefry, J., McKinley, J., Lasorsa, B., Trocine, R., 2007. In: Study of Barite Solubility and the Release of Trace Components to the Marine Environment. OCS Study MMS, 61. US Department of the Interior, Minerals Management Service, Gulf of Mexico Region, New Orleans (LA), pp. 1–147.

Davies-Colley, R., Smith, D., 2001. Turbidity, suspended sediment and water quality: a review. J. Am. Water Works Assoc. 37, 1085–1101.

De'Ath, G., 2002. Multivariate regression trees: a new technique for modeling species–environment relationships. Ecology 83, 1105–1117. https://doi.org/10.1890/0012-9658(2002)083[1105:MRTANT]2.0.CO;2.

Deltares, 2011. DELFT3D-FLOW. Simulation of Multi-dimensional Hydrodynamic Flows and Transport Phenomena, Including Sediments. Deltares Rotterdamseweg, The Netherlands.

DEWHA, 2008. In: Department of the Environment, Water, Heritage and the Art (DEWHA). Northwest Marine Bioregional Plan, Bioregional Profile. Department of the Environment, Water, Heritage and the Arts, p. 288. ISBN: 978-642-55448-2.

Durgut, I., Rye, H., Reed, M., Smit, M.G.D., Ditlevsen, M.K., 2015. Dynamic modeling of environmental risk associated with drilling discharges to marine sediments. Mar. Pollut. Bull. 99, 240–249. https://doi.org/10.1016/j.marpolbul.2015.07.019.

Edge, K.J., Johnston, E.L., Dafforn, K.A., Simpson, S.L., Kutti, T., Bannister, R.J., 2016. Sub-lethal effects of water-based drilling muds on the deep-water sponge Geodia barretti. Environ. Pollut. 212, 525–534. https://doi.org/10.1016/j.envpol.2016.02.047.

Egbert, G.D., Erofeeva, S.Y., 2002. Efficient inverse modeling of barotropic ocean tides. J. Atmos. Ocean. Technol. 19, 183–204.

Ellis, J.I., Fraser, G., Russell, J., 2012. Discharged drilling waste from oil and gas platforms and its effects on benthic communities. Mar. Ecol. Prog. Ser. 456, 285–302. https://doi.org/10.3354/meps09622.

EPA, 2011. In: Environmental Assessment Guideline for Marine Dredging Programs (EAG7). Environmental Protection Authority (EPA), Perth, Western Australia, p. 36.

Falkner, I., Whiteway, T., Przeslawski, R., Heap, A., 2009. In: Review of Ten Key Ecological Features (KEFs) in the Northwest Marine Region. Record 2009/13. Geoscience Australia, Canberra, Australia, p. 117.

Fisher, R., Stark, C., Ridd, P., Jones, R., 2015. Spatial patterns in water quality changes during dredging in tropical environments. PLoS One 10 (12), e0143309. https://doi.org/10.1371/journal.pone.0143309.

Frost, T.K., Myrhaug, J.L., Ditlevsen, M.K., Rye, H., 2014. In: Environmental Monitoring and Modeling of Drilling Discharges at a Location With Vulnerable Seabed Fauna: Comparison Between Field Measurements and Model Simulations, SPE International Conference on Health, Safety, and Environment. Society of Petroleum Engineers, Long Beach, California, USA, p. 16.

Gibbs, R.J., Matthews, M.D., Link, D.A., 1971. The relationship between sphere size and settling velocity. J. Sediment. Res. 41, 7–18.

Harvey, E., Fletcher, D., Shortis, M., 2002. Estimation of reef fish length by divers and by stereo-video: a first comparison of the accuracy and precision in the field on living fish under operational conditions. Fish. Res. 57, 255–265.

Hayes, K.R., Dambacher, J.M., Hosack, G.R., Bax, N.J., Dunstan, P.K., Fulton, E.A., Thompson, P.A., Hartog, J.R., Hobday, A.J., Bradford, R., Foster, S.D., Hedge, P., Smith, D.C., Marshall, C.J., 2015. Identifying indicators and essential variables for marine ecosystems. Ecol. Indic. 57, 409–419. https://doi.org/10.1016/j.ecolind.2015.05.006.

Heyward, A., Jones, R., Meeuwig, J., Burns, K., Radford, B., Colquhoun, J., Cappo, M., Case, M., O'Leary, R., Fisher, R., Meekan, M., Stowar, M., 2012. Montara: 2011 Offshore banks assessmenet survey. In: Final report for PTTEP Australasia (Ashmore Cartier) Pty. Ltd. Australian Institute of Marine Science (AIMS), Townsville, Australia, p. 236 pp.

Hinwood, J., Potts, A., Dennis, L., Carey, J., Houridis, H., Bell, R., Thomson, J., Boudreau, P., Ayling, A., 1994. Drilling activities. In: Swan, J., Neff, J., Young, P. (Eds.), Environmental Implications of Offshore Oil and Gas Development in Australiai. Australian Petroleum and Exploration Association, Sydney, pp. 123–207.

Holdway, D.A., 2002. The acute and chronic effects of wastes associated with offshore oil and gas production on temperate and tropical marine ecological processes. Mar. Pollut. Bull. 44, 185–203. https://doi.org/10.1016/S0025-326X(01)00197-7.

Hughes, S.J.M., Jones, D.O.B., Hauton, C., Gates, A.R., Hawkins, L.E., 2010. An assessment of drilling disturbance on Echinus acutus var. norvegicus based on in-situ observations and experiments using a remotely operated vehicle (ROV). J. Exp. Mar. Biol. Ecol. 395, 37–47. https://doi.org/10.1016/j.jembe.2010.08.012.

International Risk Consultants, 2007. Retrieved from:. In: Petroleum and Minerals Industries in the North West Region. A Report to the Department of the Environment, Water, Heritage and the Arts. Australian Government Parks Australia, p. 126 https://parksaustralia.gov.au/marine/management/resources/scientific-publications/petroleum-and-minerals-industries-north-west-marine-region/.

IOGP, 2003. In: Environmental Aspects of the Use and Disposal of Non Aqueous Drilling Fluids Associated With Offshore Oil & Gas Operations. Report 342. Version 1. International Association of of Oil and Gas Producers, p. 114. https://www.iogp.org.

IOGP, 2016. In: Environmental Fate and Effects of Ocean Discharge of Drill Cuttings and Associated Drilling Fluids From Offshore Oil and Gas Operations. Report 543. Version 1. International Association of of Oil and Gas Producers, p. 144. https://www.iogp.org.

IOGP, 2021. In: Environmental Effects and Regulation of Offshore Drill Cuttings Discharges. Report 602. Version 1. International Association of Oil and Gas Producers, p. 56. https://www.iogp.org.

Jensen, S., Högström, A., Almond, J., Taylor, W., Meinhold, G., Høyberget, M., Ebbestad, J., Agic, H., Palacios, T., 2018. Scratch circles from the Ediacaran and Cambrian of Arctic Norway and southern Africa, with a review of scratch circle occurrences. Bull. Geosci. 93 https://doi.org/10.3140/bull.geosci.1685.

Jirka, G.H., 2006. Integral model for turbulent buoyant jets in unbounded stratified flows part 2: plane jet dynamics resulting from multiport diffuser jets. Environ. Fluid Mech. 6, 43–100.

Jones, D.O., Gates, A.R., Lausen, B., 2012. Recovery of deep-water megafaunal assemblages from hydrocarbon drilling disturbance in the Faroe- Shetland Channel. Mar. Ecol. Prog. Ser. 461, 71–82. https://doi.org/10.3354/meps09827.

Jones, R., Bessell-Browne, P., Fisher, R., Klonowski, W., Slivkoff, M., 2016. Assessing the impacts of sediments from dredging on corals. Mar. Pollut. Bull. 102, 9–29. https://doi.org/10.1016/j.marpolbul.2015.10.049.
Jonker, M., Johns, K., Osborne, K., 2008. Surveys of benthic reef communities using underwater digital photography and counts of juvenile corals. In: Long-term Monitoring of the Great Barrier Reef. Standard Operational Procedure No. 10. Australian Institute of Marine Science (AIMS), Townsville, Queensland, Australia, p. 7.
Junttila, J., Dijkstra, N., Aagaard-Sørensen, S., 2018. Spreading of drill cuttings and sediment recovery of three exploration wells of different ages, SW Barents Sea, Norway. Mar. Pollut. Bull. 135, 224–238. https://doi.org/10.1016/j.marpolbul.2018.06.064.
Kahng, S., Akkaynak, D., Shlesinger, T., Hochberg, E., Wiedenmann, J., Tamir, R., Tchernov, D., 2019. Light, temperature, photosynthesis, heterotrophy, and the lower depth limits of mesophotic coral ecosystems. In: Loya, Y., Puglise, K., Bridge, T. (Eds.), Mesophotic Coral Ecosystems. Coral Reefs of the World, 12. Springer, New York, New York, USA, pp. 801–828.
Kahng, S., Copus, J., Wagner, D., 2014. Recent advances in the ecology of mesophotic coral ecosystems (MCEs). Curr. Opin. Environ. Sustain. 7, 72–81. https://doi.org/10.1016/j.cosust.2013.11.019.
Kench, P.S., McLean, R.F., 1997. A comparison of settling and sieve techniques for the analysis of bioclastic sediments. Sediment. Geol. 109, 111–119.
Kennicutt, M., Keeney-Kennicutt, W., Bresley, B., Fenner, F., 1982. The use of pyrolysis and barium distributions to assess the areal extent of drilling fluids in surficial marine sediments. Environ. Geol. 4, 239–249.
Khondaker, A., 2000. Modeling the fate of drilling waste in marine environment — an overview. Comput. Geosci. 26, 531–540. https://doi.org/10.1016/S0098-3004(99)00135-1.
Kirk, J., 1994. Light and Photosynthesis in Aquatic Ecosystems, Third edition. Cambridge University Press, New York, US. Third Edition ed.
Kramer, J., Grundy, H., Hamer, L., 1980. Occurrence and solubility of trace metals in barite for ocean drilling operations. In: Symposium on Research on Environmental Fate and Effects of Drilling Fluids and Cuttings. American Petroleum Institute, Washington DC, US, pp. 21–24.
Langlois, T., Goetze, J., Bond, T., Monk, J., Abesamis, R.A., Asher, J., Barrett, N., Bernard, A.T., Bouchet, P.J., Birt, M.J., 2020. A field and video annotation guide for baited remote underwater stereo-video surveys of demersal fish assemblages. Methods Ecol. Evol. 11, 1401–1409.
Langlois, T., Williams, J., Monk, J., Bouchet, P., Currey, L., Goetze, J., Harasti, D., Huveneers, C., Malcolm, H., Whitmarsh, S., 2018. Marine sampling field manual for benthic stereo BRUVS (Baited Remote Underwater Videos). In: Przeslawski, R., Foster, S. (Eds.), Field Manuals for Marine Sampling to Monitor Australian Waters. National Environmental Science Programme (NESP), pp. 82–104.
Larsson, A.I., van Oevelen, D., Purser, A., Thomsen, L., 2013. Tolerance to long-term exposure of suspended benthic sediments and drill cuttings in the cold-water coral Lophelia Pertusa. Mar. Pollut. Bull. 70, 176–188. https://doi.org/10.1016/j.marpolbul.2013.02.033.
Lesser, M.P., Slattery, M., Leichter, J.J., 2009. Ecology of mesophotic coral reefs. J. Exp. Mar. Biol. Ecol. 375, 1–8. https://doi.org/10.1016/j.jembe.2009.05.009.
Leuterman, A., Still, I., Johnson, I., Christie, J., Butcher, N., 1997. A study of trace metals from barites: their concentration, bioavailability, and potential for bioaccumulation. In: Proceedings of the Offshore Mediterranean Conference and Exhibition, OMC97. OMC Ravenna (IT), pp. 19–21.
Long, E.R., Macdonald, D.D., Smith, S.L., Calder, F.D., 1995. Incidence of adverse biological effects within ranges of chemical concentrations in marine and estuarine sediments. Environ. Manag. 19, 81–97.
Loya, Y., Eyal, G., Treibitz, T., Lesser, M.P., Appeldoorn, R., 2016. Theme section on mesophotic coral ecosystems: advances in knowledge and future perspectives. Coral Reefs 35, 1–9. https://doi.org/10.1007/s00338-016-1410-7.
May, R.F., 1992. Marine conservation reserves, petroleum exploration and development, and oil spills in coastal waters of Western Australia. Mar. Pollut. Bull. 25, 147–154. https://doi.org/10.1016/0025-326X(92)90218-U.
Melton, H., Smith, J., Martin, C., Nedwed, T., Mairs, H., Raught, D., 2000. In: Offshore Discharge of Drilling Fluids and Cuttings–A Scientific Perspective on Public Policy, Rio Oil and Gas Conference, 16-19 October 2000, Rio de Janeiro, Brazil, p. 13 pp.
Moore, C., Cappo, M., Radford, B., Heyward, A., 2017. Submerged oceanic shoals of North Western Australia are a major reservoir of marine biodiversity. Coral Reefs 36, 719–734.
Morelissen, R., van der Kaaij, T., Bleninger, T., 2013. Dynamic coupling of near field and far field models for simulating effluent discharges. Water Sci. Technol. 67, 2210–2220.
National Research Council (US), 1983. Panel on Assessment of Fates Effects of Drilling Fluids Cuttings in the Marine Environment. Drilling Discharges in the Marine Environment. National Academy Press, Washington DC, US.
Nedwed, T., 2004. Best practices for drill cuttings & mud discharge modeling, 29-31 March 2004. In: Proceedings: 7th SPE International Conference on Health, Safety, and Environment in Oil and Gas Exploration and Production. Society of Petroleum Engineers, Calgary, Alberta, Canada, p. 6. pp.
Nedwed, T., Smith, J.P., Melton, R., 2006. Fate of Nonaqueous Drilling Fluid Cuttings Discharged From a Deepwater Exploration Well, SPE International Health, Safety & Environment Conference. Society of Petroleum Engineers.
Neff, J., 1987. Biological effects of drilling fluids, drill cuttings and produced waters. In: Boesch, D., Rabalais, N. (Eds.), Long-term Environmental Effects of Offshore Oil and Gas Development. Elsevier Applied Science, London, UK, pp. 469–538.
Neff, J., 2010. Fate and effects of water based drilling muds and cuttings in cold water environments. In: A Scientific Review prepared for Shell Exploration and Production Company. Shell Exploration and Production Company, Houston, Texas, US.
Neff, J.M., 2002a. In: Bioaccumulation in Marine Organisms: Effect of Contaminants From Oil Well Produced Water. Elsevier, Amsterdam, The Netherlands, p. 452.
Neff, J.M., 2002b. Fates and effects of mercury from oil and gas exploration and production operations in the marine environment. In: Prepared Under Contract for American Petroleum Institute and the Ad Hoc Upstream Industry Mercury Working Group.
Neff, J.M., 2008. Estimation of bioavailability of metals from drilling mud barite. Integr. Environ. Assess. Manag. 4, 184–193.
Niu, H., Drozdowski, A., Husain, T., Veitch, B., Bose, N., Lee, K., 2009. Modeling the dispersion of drilling muds using the bblt model: the effects of settling velocity. Environ. Model. Assess. 14, 585–594. https://doi.org/10.1007/s10666-008-9162-6.
Niu, H., Lee, K., 2013. Refinement and Validation of Numerical Risk Assessment Models for Use in Atlantic Canada. Environmental Studies Research Funds.
NOPSEMA, (2018). Oil Pollution Risk Management. Guidance Note. GN1488 Rev 2, February 2018. National Offshore Petroleum Safety and Environmental Management Authority (NOPSEMA), Perth, Western Australia. pp. 33. https://www.nopsema.gov.au/assets/Guidance-notes/A382148.pdf.
O'Brien, G., Glenn, K., Lawrence, G., Williams, A., Webster, M., Burns, S., Cowley, R., 2002. Influence of hydrocarbon migration and seepage on benthic communities in the Timor Sea, Australia. APPEA J. 42, 225–240.
Oksanen, J., Blanchet, G., Friendly, M., Kindt, R., Legendre, P., McGlinn, D., Minchin, P., O'Hara, R., Simpson, G., Solymos, P., Stevens, M., Szoecs, E., Wagner, H., 2018. Vegan: community ecology package, R package version 2.5-2. https://CRAN.R-project.org/package=vegan. Vie Milieu.
Phillips, C., Evans, J., Hom, W., Clayton, J., 1998. Long-term changes in sediment barium inventories associated with drilling-related discharges in the Santa Maria Basin, California, USA. Environ. Toxicol. Chem. 17, 1653–1661.
Pineda, M.-C., Strehlow, B., Sternel, M., Duckworth, A., Haan, J.d., Jones, R., Webster, N. S., 2017a. Effects of sediment smothering on the sponge holobiont with implications for dredging management. Sci. Rep. 7, 5156. https://doi.org/10.1038/s41598-017-05243-x.
Pineda, M.-C., Strehlow, B., Sternel, M., Duckworth, A., Jones, R., Webster, N., 2017b. Effects of suspended sediments on the sponge holobiont with implications for dredging management. Sci. Rep. 7, 4925. https://doi.org/10.1038/s41598-017-05241-z.
Pivel, M., Freitas, C., Comba, J., 2009. Modeling the discharge of cuttings and drilling fluids in a deep-water environment. Deep-Sea Res. II Top. Stud. Oceanogr. 56, 12–21.
Priede, I., Bagley, P., Smith, A., Creasey, S., Merrett, N., 1994. Scavenging deep demersal fishes of the porcupine seabight, north-East Atlantic: observations by baited camera, trap and trawl. J. Mar. Biol. Assoc. U. K. 74, 481–498.
Purser, A., 2015. A time series study of Lophelia Pertusa and reef megafauna responses to drill cuttings exposure on the norwegian margin. PLoS One 10, e0134076.
R Core Team, 2017. R: A Language and Environment for Statistical Computing. URL. R Foundation for Statistical Computing, Vienna, Austria. https://www.R-project.org/.
Rhoads, D., 1974. Organism-sediment relations on the muddy sea floor. Oceanogr. Mar. Biol. 12, 263–300.
Richert, C., Rogers, A., Burton, M., 2015. Measuring the extent of a social license to operate: the influence of marine biodiversity offsets in the oil and gas sector in Western Australia. Resour. Policy 43, 121–129. https://doi.org/10.1016/j.resourpol.2014.12.001.
Roos, P.C., Blondeaux, P., 2001. Sand ripples under sea waves. Part 4. Tile ripple formation. J. Fluid Mech. 447, 227–246.
Rye, H., Furuholt, E., 2010. In: Validation of a Numerical Model for Simulation of Drilling Discharges to Sea, Abu Dhabi International Petroleum Exhibition and Conference UAE, 1-4 November 2010. Society of Petroleum Engineers, p. 12.
Rye, H., Loekken, M., Moe, J., Ditlevsen, M.K., 2012. In: Simulation of Concentrations and Depositions of Particle Matter Caused by Drilling Discharges. Comparison Between Field Measurements and Simulation Results at Coral Locations, International Conference on Health, Safety and Environment in Oil and Gas Exploration and Production. Society of Petroleum Engineers, Perth, Australia, p. 15.
Rye, H., Reed, M., Frost, T.K., Røe Utvik, T.I., 2006. Comparison of the ParTrack mud/cuttings release model with field data based on use of synthetic-based drilling fluids. Environ. Model Softw. 21, 190–203. https://doi.org/10.1016/j.envsoft.2004.04.018.
Rye, H., Reed, M., Frost, T.K., Smit, M.G., Durgut, I., Johansen, Ø., Ditlevsen, M.K., 2008. Development of a numerical model for calculating exposure to toxic and nontoxic stressors in the water column and sediment from drilling discharges. Integr. Environ. Assess. Manag. 4, 194–203.
Schaanning, M.T., Trannum, H.C., Øxnevad, S., Carroll, J., Bakke, T., 2008. Effects of drill cuttings on biogeochemical fluxes and macrobenthos of marine sediments. J. Exp. Mar. Biol. Ecol. 361, 49–57.
Schobernd, Z., Bacheler, N., Conn, P., 2014. Examining the utility of alternative video monitoring metrics for indexing reef fish abundance. Can. J. Fish. Aquat. Sci. 71, 464–471. https://doi.org/10.1139/cjfas-2013-0086.
Schonberg, C., Fromont, J., 2014. Sponge functional growth forms as a means for classifying sponges without taxonomy. In: The Ningaloo Atlas. http://ningaloo-atlas.org.au/content/sponge-functional-growth-forms-means-classifying-spo.
Simpson, S., Batley, G., Chariton, A., 2013. Revision of the ANZECC/ARMCANZ sediment quality guidelines. In: CSIRO Land and Water Science Report 08/07., CSIRO Land and Water, p. 132. https://doi.org/10.4225/08/5894c6184320c.
Smit, M., Holthaus, K.I.E., Trannum, H.C., Neff, J.M., Kjeilen-Eilertsen, G., Jak, R.G., Singsaas, I., Huijbregts, M.A.J., Hendriks, A.J., 2008. Species sensitivity distributions

for suspended clays, sediment burial, and grain size change in the marine environment. Environ. Toxicol. Chem. 27, 1006–1012. https://doi.org/10.1897/07-339.1.

Sun, C., Branson, P., 2019. Numerical modelling of dredge plumes. In: Report of Theme 3 - Project 3.4. Prepared for the Dredging Science Node, Western Australian Marine Science Institution. Perth, Western Australia, p. 84.

Vad, J., Kazanidis, G., Henry, L.-A., Jones, D.O.B., Tendal, O.S., Christiansen, S., Henry, T.B., Roberts, J.M., 2018. Potential impacts of offshore oil and gas activities on Deep-Sea sponges and the habitats they form. Adv. Mar. Biol. 79, 33–60. https://doi.org/10.1016/bs.amb.2018.01.001.

Van Rijn, L., 2007. Principles of Sediment Transport in Rivers, Estuaries, and Coastal Seas (Update 2006). Aqua Publications, Blokzijl, The Netherlands. www.aquapublications.nl.

Vince, J., Smith, A.D.M., Sainsbury, K.J., Cresswell, I.D., Smith, D.C., Haward, M., 2015. Australia's oceans policy: past, present and future. Mar. Policy 57, 1–8. https://doi.org/10.1016/j.marpol.2015.02.014.

Whinney, J., Jones, R., Duckworth, A., Ridd, P., 2017. Continuous in situ monitoring of sediment deposition in shallow benthic environments. Coral Reefs 36, 521–533. https://doi.org/10.1007/s00338-016-1536-7.

Whitmarsh, S.K., Fairweather, P.G., Huveneers, C., 2017. What is big BRUVver up to? Methods and uses of baited underwater video. Rev. Fish Biol. Fish. 27, 53–73.

Willis, T.J., Babcock, R.C., 2000. A baited underwater video system for the determination of relative density of carnivorous reef fish. Mar. Freshw. Res. 51, 755–763. https://doi.org/10.1071/MF00010.

Wilson, B., 2013. The Biogeography of the Australian North West Shelf: Environmental Change and Life's Response. Elsevier, Burlington, MA, US. ISBN 9780124095168.

Wilson, S., Kendrick, A., Wlison, B., 2019. The North-Western margin of Australia. Chapter 14. Volume II: The Indiian ocean to the pacific. In: Sheppard, C. (Ed.), World Seas: An Environmental Evaluation, 2nd edition. Academic Press, pp. 303–314.

Zhao, L., Chen, Z., Lee, K., 2011. Modelling the dispersion of wastewater discharges from offshore outfalls: a review. Environ. Rev. 19, 107–120.